Biochemistry

Article

Comparison of the kinase profile of midostaurin (Rydapt®) with that of its predominant metabolites

Paul William Manley, Giorgio Caravatti, Pascal Furet, Johannes Roesel, Phi Tran, Trixie Wagner, and Markus Wartmann

Biochemistry, **Just Accepted Manuscript** • DOI: 10.1021/acs.biochem.8b00727 • Publication Date (Web): 27 Aug 2018

Just Accepted

ACS Publications

is published by the American Chemical Society. 1155 Sixteenth Street N.W., Washington, DC 20036

Comparison of the kinase profile of midostaurin (Rydapt®) with that of its predominant metabolites and the potential relevance of some newly identified targets to leukemia therapy

Paul W. Manley,[*,†] Giorgio Caravatti,[†] Pascal Furet,[†] Johannes Roesel,[‡] Phi Tran,[§] Trixie Wagner,[†] and Markus Wartmann[‡]

[†]Global Discovery Chemistry, Novartis Institutes for Biomedical Research, Novartis International AG, CH-4002 Basel, Switzerland

[‡]Oncology Disease Area, Novartis Institutes for Biomedical Research, Novartis International AG, CH-4002 Basel, Switzerland

[§]Department of Drug Metabolism and Pharmacokinetics, Novartis Institutes for Biomedical Research, East Hanover, New Jersey 07936, United States

ABSTRACT: The multi-targeted protein kinase inhibitor midostaurin is approved for the treatment of both newly-diagnosed FLT3-mutated acute myeloid leukemia (AML) and KIT-driven advanced systemic mastocytosis (SM). AML is a heterogeneous malignancy and investigational drugs targeting FLT3 have shown disparate effects in patients with FLT3-mutated AML, probably as a result of their inhibiting different targets and pathways at the administered doses. However, the efficacy and side-effects of drugs do not just reflect the biochemical and pharmacodynamic properties of the parent compound, but are often comprised of complex cooperative effects between the properties of the parent and active metabolites. Following chronic dosing, two midostaurin metabolites attain steady-state plasma trough levels greater than that of the parent drug. In this study we characterised these metabolites and determined their profiles as kinase inhibitors using radiometric transphosphorylation assays. Like midostaurin the metabolites potently inhibit mutant forms of FLT3 and KIT, as well as several additional kinases that are either directly involved in the deregulated signaling pathways or which have been implicated as playing a role in AML via stromal support, such as IGF1R, LYN, PDPK1, RET, SYK, TRKA and VEGFR2. Consequently, a complex interplay between the kinase activities of midostaurin and its metabolites is likely to contribute to the efficacy of midostaurin in AML and helps to engender the distinctive effects of the drug compared to other FLT3 inhibitors in this malignancy.

INTRODUCTION

Often the efficacy and side-effects of drugs do not only reflect the biochemical and pharmacodynamic properties of the parent molecule, but result from complex cooperative effects between the properties of the parent and its active metabolites. This aspect is often overlooked when attempts are made to assign class effects for both efficacy and adverse-events to a group of drugs, which is particularly the case for protein kinase inhibitors. The human kinome has a full complement 538 genes [http://kinase.com/web/current/], most (≥478) of which encode protein kinases with catalytic domains whose sequences are closely-related.[1,2] These protein kinases, which can be clustered into groups based upon sequence similarity and biochemical function, catalyse the transfer of the terminal phosphate group of adenosine triphosphate (ATP) onto the side-chain hydroxy groups of either serine, threonine or tyrosine residues in substrate proteins, thereby playing a crucial role in the multitude of signal transduction pathways that regulate the functions of all eukaryotic cells. Drugs designed to target one or more particular protein kinases in order to elicit a desired pharmacological effect are rarely specific, but have distinct inhibition profiles both within and across the different groups of protein kinases. Consequently, it is extremely difficult to assign class effects to drugs acting upon protein kinases.

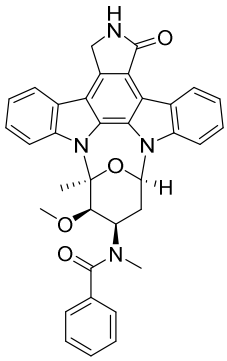

1 (midostaurin; PKC412)

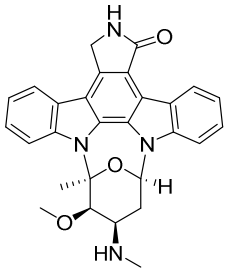

2 (staurosporin)

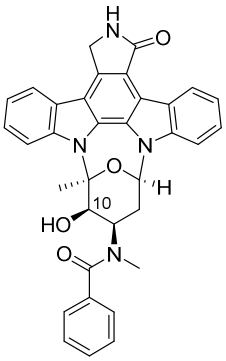

3 (CGP62221: 10-*O*-desmethyl)

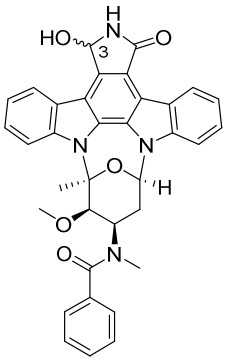

4 (e1: 3-*S*-hydroxy)
5 (e2: 3-*R*-hydroxy)
[e1+e2] (CGP52421; (±)-3-hydroxy)

Figure 1. Structures of midostaurin (**1**), staurosporine (**2**) and the primary metabolites of midostaurin: CGP62221 (**3**), e1 (**4**) and e2 (**5**). Whereas the 1:1 mixture of e1 and e2 of was previously designated CGP52421, the definitive stereochemistry of the two epimeric C3-hydroxylated compounds has been established in the present study.

This situation applies to midostaurin (**1**; Rydapt®; Figure 1), a drug recently approved by health authorities for the treatment of two malignancies: (i) acute myeloid leukemia (AML) in newly diagnosed patients who are FMS-like tyrosine kinase 3 (FLT3) mutation-positive, in combination with chemotherapy;[3] (ii) as monotherapy in advanced systemic mastocytosis (SM), which includes aggressive systemic mastocytosis, systemic mastocytosis with associated haematological neoplasm and mast cell leukemia.[4] Although the activity of midostaurin in SM most likely results from targeting the oncogenic D816V mutant form of the stem cell factor receptor tyrosine kinase (KIT),[5] as will be discussed in this article, the efficacy of midostaurin in AML patients is probably a consequence of the inhibition of multiple kinases including FLT3, by both the parent compound and several of its metabolites.

Among the first natural products to be discovered as inhibitors of protein kinases,[6-9] the bacterial alkaloid staurosporine (**2**; Figure 1) was initially found to be a potent inhibitor of the PKC family of phospholipase-dependent kinases,[10] although it was later shown to inhibit and/or bind to many members of the human kinome.[9,11,12] With this knowledge staurosporine served as a lead compound for a drug discovery programme for PKC inhibitors,[13] which culminated in 1986 with the discovery of midostaurin.[14] Based upon the then known biochemical and pharmacological profile of the drug as both an anti-tumour and anti-angiogenic agent,[15,16] midostaurin was advanced into Phase 1 clinical trials as an anti-cancer agent and as a treatment for diabetic macular edema.[17,18]

During the course of these studies it was recognised that the presence of mutant forms of the FLT3 transmembrane receptor kinase in the leukemic cells of AML patients was associated

with poor prognosis.[19-25] These mutations comprise of either internal tandem duplications (ITD) at various positions and of varying length (up to 100 amino-acids) within the juxtamembrane domain that compromise the autoregulatory mechanism of FLT3,[25] or of amino-acid substitutions of the activation loop Asp835 residue that destabilise the inactive conformation of the kinase domain.[26]. These mutations render the receptor kinase constitutively active, such that it is no longer dependent upon extracellular engagement of the FLT3L growth factor to drive the cell cycle progression and proliferation of the transformed haematopoietic cells.[24] These findings prompted the search for FLT3 kinase inhibitors as potential therapies for AML.[27,28] Midostaurin was duly found to be a potent inhibitor of *wild-type* as well as ITD and D835Y mutant forms of FLT3, and this activity translated into efficacy in FLT3-dependent myeloproliferative disease models in mice.[29] Based upon these findings, midostaurin was advanced into clinical trials in both AML and myelodysplastic syndrome (MDS) patients who harboured either *wild-type* or mutated FLT3, where it was demonstrated to have single agent activity.[30] Subsequently a Phase 3 trial in patients aged 18-60 years having AML harbouring activating FLT3 mutations, showed that addition of midostaurin (50 mg, BID) to standard chemotherapy significantly improved event-free survival and overall survival compared to standard chemotherapy,[3,31] thereby leading to health authority approvals of the drug in 2017.

From clinical studies it has now been established that midostaurin undergoes extensive metabolism by the hepatic CYP3A4 enzyme into three primary metabolites: the 10-O-demethylated compound CGP62221 (**3**) and two epimeric C3-hydroxylated compounds, e1 (**4**) and e2 (**5**) (Figure 1), with the definitive stereochemistry of these being established in the present study (previously the e1 + e2 mixture of was designated CGP52421). Thus, following the administration of a single 50 mg dose of [^{14}C]-labelled drug to fasted, healthy adults (n = 6), midostaurin, CGP62221, e1 and e2 accounted for 22%, 28%, 5.3% and 33% of the total drug-related mean plasma $AUC_{0\text{-}96hr}$ respectively,[32] and in diabetes patients (n = 9), following

50 mg BID the mean plasma trough levels on day 28 of midostaurin, CGP62221 and e2 were 0.82, 1.48 and 6.73 μM.[33] These findings have been further substantiated in AML patients, where following 50 mg BID the mean steady-state plasma trough levels of midostaurin, CGP62221 and [e1 + e2] were 1.25 ± 0.35, 2.08 ± 0.29 and 9.61 ± 1.16 μM, confirming substantial accumulation of e2 but, as indicated from a single patient, not e1.[29,34]

In addition to midostaurin, other indolocarbazole-type pan-kinase inhibitors, as well as structurally diverse agents with varying degrees of selectivity towards FLT3 have been evaluated in clinical trials (Figure 2), and these have been found to elicit quite disparate effects.[35-37] Therefore it is important to investigate the potential mechanisms of actions of midostaurin that contribute to its efficacy in AML. In this study we compare the kinase profile of midostaurin with that of its predominant metabolites and discuss our findings.

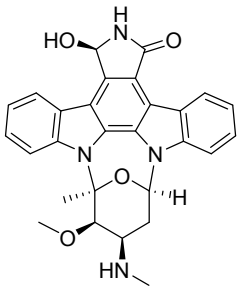

UCN-01
(Kyowa Hakko Kirin)

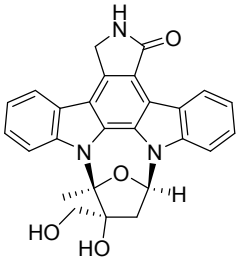

Lestauritinib; CEP701
(Kyowo Hakko Kirin / Cephalon)

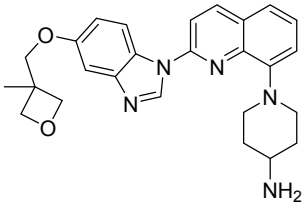

Crenolanib
(Arog)

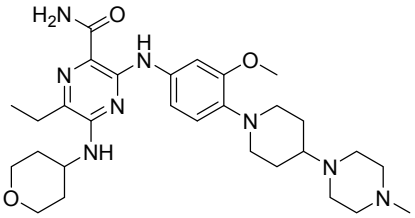

Gilteritinib; ASP2215
(Kotobuki / Astellas)

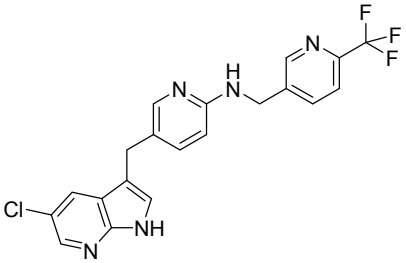

Pexidartinib; PLX3397
(Plexxikon)

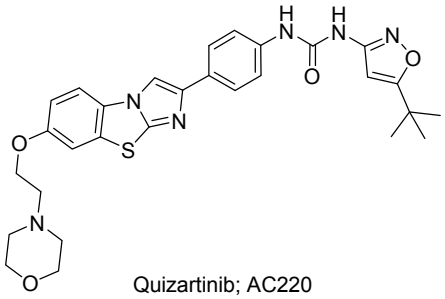

Quizartinib; AC220
(Ambit / Daiichi Sankyo)

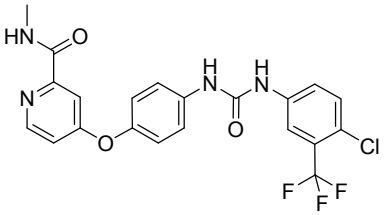

Sorafenib; BAY43-9006
(Bayer)

Figure 2. Structures of investigational ATP-competitive FLT3 kinase inhibitors studied in AML patients. Like midostaurin, UCN-01, lestauritinib and crenolanib are type-1 inhibitors binding to the active conformation of FLT3,[38] whereas quizartinib, pexidartinib and sorafenib bind to an inactive conformation in a type-2 fashion.

EXPERIMENTAL DETAILS

Preparation and characterization of compounds:

***N*-[(9*S*,10*R*,11*R*,13*R*)-2,3,10,11,12,13-hexahydro-10-methoxy-9-methyl-1-oxo-9,13-epoxy-1*H*,9*H*-diindolo[1,2,3-*gh*:3',2',1'-*lm*]pyrrolo[3,4-*j*][1,7]benzodiazonin-11-yl]-*N*-methylbenzamide** (**1**; midostaurin) was prepared as an amorphous solid by benzoylation of **2** as described;[39] 1H NMR (600 MHz, DMSO-d6) δ 1.98 (br s, 1H), 2.41 (br s, 1H), 2.29 - 2.44 (m, 1H), 2.46 (br s, 1H), 2.51 - 2.62 (m, 1H), 2.75 (br s, 2H), 2.82 (br s, 2H), 2.83 - 2.90 (m, 2H), 4.51 (br s, 1H), 5.00 (br s, 2H), 7.08 - 7.12 (m, 1H), 7.30 (t, J=7.76 Hz, 1H), 7.37 (t, J=7.62 Hz, 1H), 7.43 (br s, 1H), 7.47 (br s, 1H), 7.47 - 7.57 (m, 3H), 7.63 (br s, 2H), 7.69 (br s, 1H), 8.07 (d, J=7.89 Hz, 2H), 8.63 (s, 1H), 9.29 (d, J=8.04 Hz, 1H). Solubility (shake-flask method) at pH 1.0 and 6.8 (25°C): 0.3 and 0.1 μg/L respectively.

***N*-[(9*S*,10*R*,11*R*,13*R*)-2,3,10,11,12,13-hexahydro-10-hydroxy-9-methyl-1-oxo-9,13-epoxy-1*H*,9*H*-diindolo[1,2,3-*gh*:3',2',1'-*lm*]pyrrolo[3,4-*j*][1,7]benzodiazonin-11-yl]-*N*-methylbenzamide** (**3**; CGP62221). A mixture of (9*S*,10*R*,11*R*,13*R*)-2,3,10,11,12,13-hexahydro-10-hydroxy-9-methyl-11-(methylamino)-9,13-epoxy-1*H*,9*H*-diindolo[1,2,3-*gh*:3',2',1'-*lm*]pyrrolo[3,4-*j*][1,7]benzodiazonin-1-one[40] (2.47 g, 5.4 mmol) and benzoic anhydride (1.22 g, 5.4 mmol) in EtOH (65 mL of 95%) stirred at 70°C for 45 min. The solvent was evaporated off under reduced pressure and the residue was dissolved in EtOAc. The solution was washed with HCl (1 M), water, saturated aq. $NaHCO_3$ and saturated aq. NaCl, dried (Na_2SO_4) and the solvent was evaporated off under reduced pressure. The crude product was

purified by column chromatography (silica gel, 5% EtOH in CH_2Cl_2) and recrystallised from EtOH-CH_2Cl_2 to afford **3** as a colourless crystalline solid (1.41 g, 33%): m.p. 246-257°C (decomp.); 1H NMR (600 MHz, DMSO-d6) δ 9.27 (d, J=8.0 Hz, 1H), 8.60 (s, 1H), 8.04 (d, J=7.5 Hz, 1H), 7.97 (s, 1H), 7.75 (s, 1H), 7.60 (s, 2H), 7.52 – 7.42 (m, 5H), 7.34 (t, J=7.3 Hz, 1H), 7.29 (t, J=7.2 Hz, 1H), 7.12 (s, 1H), 5.78 (d, J=6.9 Hz, 1H), 4.99 (s, 3H), 4.80 (s, 1H), 2.72 (d, J=29.6 Hz, 4H), 2.38 (s, 1H), 2.26 (s, 3H). Anal. Cald. for $C_{34}H_{28}N_4O_4.0.5H_2O$: C, 72.20; H, 5.17; N, 9.90. Found: C, 72.00; H, 5.48; N, 9.62.

***N*-[(3*S*,9*S*,10*R*,11*R*,13*R*)-2,3,10,11,12,13-hexahydro-3-hydroxy-10-methoxy-9-methyl-1-oxo-9,13-epoxy-1H,9H-diindolo[1,2,3-gh:3',2',1'-lm]pyrrolo[3,4-j][1,7]benzodiazonin-11-yl]-*N*-methylbenzamide** (**4**). A solution of 2,3-dichloro-5,6-dicyano-1,4-benzoquinone (DDQ; 0.406 g, 1.75 mmol) in CH_3CN – H_20 (3.5 mL of 1:1) was added to a solution of **1** (1.00 g, 0.75 mmol) in CH_2Cl_2 (23 mL) at 20°C in the dark. The resulting green solution was stirred for 10 min and then extracted with CH_2Cl_2. The combined extracts were dried (Na_2SO_4) and solvent was evaporated off under reduced pressure. The crude mixture was purified by column chromatography (silica gel, 0-3% EtOH in EtOAc) and crystallized from dioxane-toluene to afford the less polar epimer, **4** as a colourless crystalline solid (0.32 g, 42%): m.p. 298-301°C; 1H NMR (600 MHz, DMSO-d6) δ 9.25 (dd, J=7.9, 1.1 Hz, 1H), 8.91 – 8.81 (m, 1H), 8.47 (dd, J=7.9, 1.2 Hz, 1H), 8.00 (s, 1H), 7.76 – 7.40 (m, 8H), 7.35 (t, J=7.5 Hz, 1H), 7.32 (t, J=7.8 Hz, 1H), 7.09 (s, 1H), 6.84 (s, 0H), 6.52 – 6.39 (m, 2H), 5.10 (d, J=58.7 Hz, 1H), 4.52 (s, 1H), 4.27 (d, J=90.8 Hz, 1H), 3.03 – 2.67 (m, 6H), 2.64 – 2.21 (m, 5H), 1.98 (s, 1H).

Attempts to isolate the more polar epimer, **5** resulted in epimerisation and / or formation of the 3-methoxy-derivative.

Crystal structure determination and refinement of compound 4: Diffraction data were collected with a Bruker AXS SMART 6000 CCD detector on a three-circle platform

goniometer with Cu(Ka) radiation (λ = 1.54178 Å) from a rotating anode generator equipped with Helios multilayer mirrors. A semi-empirical absorption correction (SADABS) was applied, based on the intensities of symmetry-related reflections measured at different angular settings (maximum and minimum transmission 0.6495 and 0.7531). The structure was solved by dual-space recycling methods and refined on F^2 with the SHELXTL suite of programs. Anisotropic displacement parameters were used for all non-hydrogen atoms. All hydrogen atoms were calculated in idealized positions and refined using a riding model. The final cif file was generated with shelxl 2013/4.[41] The absolute structure was determined to be C2R, C4R, C5R, C6S, C21S; Flack x = 0.06(8), based on 2479 quotients.[42]

Compound **4** crystallized in the hexagonal space group $P6_1$ with one ordered equivalent of dioxane. Additional residual electron density in a channel parallel to the crystallographic *c* axis (0, 0, z) could not be interpreted unambiguously. The contribution of the disordered solvent to the scattering factors was taken into account with PLATON/SQUEEZE.[43] A total of 145 electrons was found in the cell, corresponding to approximately three molecules of dioxane or toluene. The compound **4** to solvent ratio could then be assumed to be approximately 1:1.5. Where relevant, the crystal data reported (chemical formula, formula weight M_r, absorption coefficient μ, $F(000)$, and density D_x) are given without the contribution of the disordered solvent.

Final data: $C_{35}H_{30}N_4O_5 \cdot C_4H_8O_2$; M_r = 674.73, crystal size 0.36·0.03·0.02 mm^3, hexagonal, space group $P\,6_1$ (No. 169) with a = 19.342(5), c = 16.050(5) Å, V = 5200(3) $Å^3$, Z = 6, D_c = 1.293 $g \cdot cm^{-3}$, μ = 0.733 mm^{-1}, $F(000)$ = 2136, 78990 reflections measured, 6061 independent, R_{int} = 0.0324, 2.64º < θ < 66.53º, T = 100(2) K, 455 parameters, 1 restraint, R_1 = 0.0311, wR_2 = 0.0696 for 5640 reflections with $I > 2\sigma(I)$, R_1= 0.0351, wR_2 = 0.0709 for all 6061 data, GoF = 1.051, restrained GoF = 1.051, res. el. dens. = +0.12 / -0.14 $e \cdot Å^3$.

Structure assignment of midostaurin metabolites e1 and e2. Midostaurin was incubated with thawed, cryopreserved human hepatocytes and the incubate was characterised by ultra-high performance liquid chromatography, coupled with time-of-flight mass spectrometry (UHPLC-MS). Briefly, vials containing cryopreserved, mixed gender hepatocytes (BiorecalmationIVT, Baltimore, MD) were thawed at 37°C for 1.5 min and the contents were suspended in 48 mL of buffer (InVitroGRO HT, cat. #Z99019; BiorecalmationIVT). The cells were recovered by centrifugation (80 × g for 10 min) and resuspended in a 2% mixture of modified Krebs-Henseleit buffer for hepatocyte incubation (In VitroGRO KHB, cat. # Z99074; BiorecalmationIVT) in fetal calf serum (FCS; Invitrogen, Walkersville, MD). An aliquot of the final suspension was removed for cell counting and for cell viability estimation (Nucleoconuter NC-3000). A 500 μL aliquot of the final cell suspension (~2×10^6 cells/mL) was added to one well of a 12-well plate predispensed with 0.5 mL of In VitroGRO KHB containing 2% FCS and midostaurin (10 μM) and incubated for 24 h without shaking, at 37°C in a humidified cell culture incubator (5% CO_2, 95% air). The well was emptied and washed with CH_3CN (2 mL). Aliquots (1 mL) of the combined contents and washings were centrifuged (13500 rpm for 10 min) at 10°C and evaporated to dryness (GeneVac, LTD Ipswich, UK) at 30°C. The residues were reconstituted in aqueous MeOH (200 μL of 50%) and 10 μL aliquots of the cell lysate mixture were injected into the UHPLC-MS system for analysis.

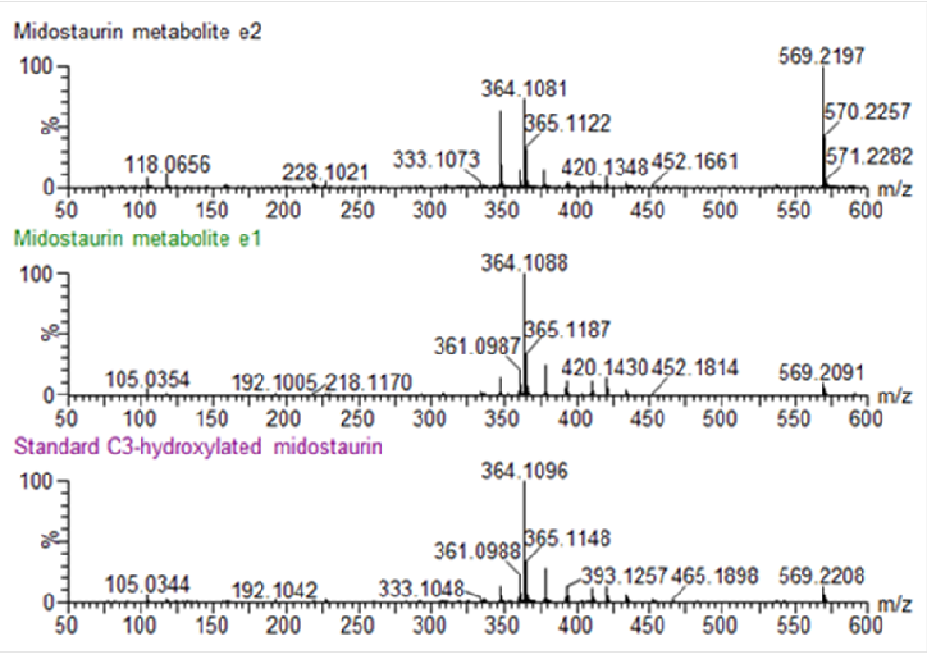

Figure 3. Ultra-high performance liquid chromatography coupled with time-of-flight mass spectrometry (UPLC-MS) evidence confirming that the less polar midostaurin metabolite e1, formed from human hepatocytes, has 3-(*R*)-stereochemistry. Top panel: Product ion mass spectra of midostaurin metabolite e2, which eluted at 24.9 minute, characterized by m/z 569 (corresponding to loss of H_2O). Middle panel: Product ion mass spectra of midostaurin metabolite e1, which eluted at 22.5 minute. Bottom panel: product ion mas spectrum synthesised standard sample of 3-(*S*)-hydroxylated compound (**4**).

The hydroxylated epimer e1 of the CGP52421 mixture eluted at 22.5 minute and epimer e2 eluted at 24.9 minute. Consistent with the ease of methoxylation discussed above, under the UPLC-MS conditions, source fragmentation (loss of water) was pronounced for e2 (Figure 3). The authentic C3-hydroxylated compound **4** had a retention time and product ion mass spectrum which exactly matched that previously identified as epimer e1 (Figure 3).

Biochemical evaluation of effects on kinase activity: The kinase profiles of compounds were determined at ProQinase GmbH (Freiburg, Germany). All kinases were produced from human cDNAs either as full-length or enzymatically active fragments, expressed in Sf9 insect cells or in

Escherichia coli as recombinant glutathione S-transferase (GST) fusion proteins or His-tagged proteins, and purified by either GSH affinity chromatography or immobilized metal affinity chromatography (affinity tags were removed from a number of kinases during purification). The purity and identity of each kinase was checked by SDS-PAGE/silver staining and by western blot analysis with specific antibodies or, in the case of lipid kinases by mass spectrometry. Kinases provided by vendors (Carna Biosciences, Inc.; Invitrogen Corp.; Millipore Corp.) were expressed, purified and quality controlled based on vendor-supplied information.

The effects of compounds on human protein kinases were assessed in radiometric assays (^{33}PanQinase®), performed using a BeckmanCoulter Biomek 2000/SL robotic system, with 96-well FlashPlates (Perkin-Elmer, Boston,MA) in a 50 µL reaction volume. The reaction cocktail was pipetted in four steps: (i) 10 µL of non-radioactive ATP solution (in H_2O); (ii) 25 µL of assay buffer–[γ-^{33}P]ATP mixture; (iii) 5 µL of test compound in 10% DMSO; (iv) 10 µL of enzyme-substrate mixture. The assay for all enzymes contained 70 mM HEPES-NaOH (pH 7.5), 3 mM $MgCl_2$, 3 µM sodium orthovanadate, 1.2 mM dithiothreitol, ATP–[γ-^{33}P]-ATP (variable amounts, corresponding to the apparent ATP Km of the respective kinase; ≈ 8 x 10^5 cpm/well), and purified protein kinase and substrate (both variable amounts). The concentrations of ATP, enzymes and substrates employed are shown in Supplementary Table 1. Additional chemicals incorporated in specific assays were as follows: All PKC assays (except for PKC-µ and -ν) also contained 1mM $CaCl_2$, 4 mM EDTA, 5 µg/mL phosphatidylserine and 1 µg/mL 1,2-dioleyl-glycerol; the CAMK-1D, -2A, -2B, -2D, -4, -K1, -K2, DAPK2, EEF2K, MYLK, MYLK2 and MYLK3 assays included 1 µg/mL calmodulin and 0.5 mM $CaCl_2$; the PRKG-1 and -2 assays contained 1 µM cGMP; the DNA pharmacokinetic (PK) assay contained 2.5 µg/mL DNA. The reaction cocktails were incubated at 30°C for 60 min and reactions then stopped by adding 50 µL of 2 % (v/v) H_3PO_4. Plates were then aspirated, washed with NaCl (2 x 200 µL 0.9 % w/v) and the incorporation of ^{33}Pi (counting of 'cpm') was determined with a microplate scintillation counter (Microbeta, Wallac). For each kinase, the median value of the

cpm of three wells was defined as 'low control' (n=3), which reflected unspecific binding of radioactivity to the plate in the absence of enzyme, but in the presence of substrate. In addition, the median value of the cpm of three other wells was taken as the 'high control', corresponding to full activity in the absence of any inhibitor (n=3). The difference between high and low control of each enzyme was taken as 100% activity. For data evaluation, the low control of each kinase was subtracted from the high control value as well as from their corresponding 'compound values' and the residual activity (in %) for each compound well was calculated by using the formula: Residual Activity (%) = 100 x [(signal of compound – low control) / (high control – low control)]. To measure IC_{50} values against selected enzymes, 10 concentrations of each compound in the 0.3 nM - 10 µM range were used and values were calculated using Quattro Workflow V3.1.1 (Quattro Research GmbH, Munich, Germany). The fitting method was a least-squares fit based upon the 'sigmoidal response (variable slope)' with parameters 'top' fixed at 100% and 'bottom' at 0%.

Effects on lipid kinase activity were assessed using a non-radiometric ADP-Glo™ Assay (Promega, Madison, Wi, USA) performed in 96-well half-area microtiter plates (Greiner Bio-One, Frickenhausen, Germany) in a 25 µL reaction volume. The reaction cocktail was pipetted sequentially: (i)10 µL of ATP solution (variable concentrations, corresponding to the apparent ATP-Km of the respective kinase) in assay buffer (50 mM HEPES-NaOH, pH 7.5, 1 mM EGTA, 100 mM NaCl, 0.03% CHAPS, 2 mM DTT; assays for PI4KB, PIK3C2A, PIK3C2B, PIK3C3, PIK3CA/PIK3R1, PIK3CD/PIK3R1 and PIK3CG additionally contained 3 mM $MgCl_2$); (ii) 5 µL of test compound (10 µM) in 10% DMSO; (iii) 10 µL of variable amounts of enzyme-substrate mixtures; the concentrations of ATP, enzymes and substrates employed are shown in Supplementary Table 1. After incubation at 30°C for 40 min, reactions were stopped with 25 µL ADP-Glo reagent per well. Plates were then incubated for 40 min at room temperature, followed by addition of 50 µL kinase detection reagent per well and incubated for a further 60 min at room temperature. Signals were measured as 'counts per

second' (cps), using a Victor2 microplate multilabel reader (Perkin Elmer, Boston, Ma, USA) in luminescence mode. For each kinase, the median cps value of three wells with complete reaction cocktails, but without kinase, was defined as 'low control'. Additionally, for each kinase the median value of the cps of three other wells with the complete reaction cocktail, but without any compound, was taken as the 'high control', *i.e.* full activity in the absence of any inhibitor. The difference between high and low control of was taken as 100% activity for each kinase. As part of the data evaluation the low control of each kinase was subtracted from the high control value as well as from their corresponding 'compound values'. The residual activity (in %) for each compound well was calculated by using the formula: Residual Activity (%) = 100 x [(cps of compound – low control) / (high control – low control)].

Evaluation of effects on proliferation / viability of human cancer cell lines: The cellular effects of midostaurin were determined on 469 commercially available human cancer cell lines (including 69 hematologic) using the cancer cell line encyclopoedia (CCLE) screen.[44] Cell-line identities were confirmed by single-nucleotide polymorphism genotyping and they were all shown to be free of mycoplasma by PCR. The screen employed the CellTiter-Glo® Luminescent Cell Viability Assay (Promega, Madison, USA) based upon quantitation of ATP as an indicator of metabolically active cells according to the published method,[44] to assess the number of viable cells in culture (appropriate media supplemented with 10% FCS) following 72 h incubation with drug in a 1536-well format. The maximum effect level (A_{max}) and the inflection point were taken from 8-point dose-response curves, several of which are illustrated in Supplemental Figure S1, and the results are summarised in Figure 4.

Evaluation of effects on proliferation / viability of kinase dependent cell lines: The potential for compounds to inhibit particular kinases in a cellular context was further quantified in the BaF3 assay system consisting of *wild-type* IL-3-dependent hematopoietic BaF3 cell models rendered IL-3 independent by transduction with various constitutively

active tyrosine kinases,[45] and in human cell lines carrying oncogenic kinases. BaF3-BCR-ABL1 cells were obtained by transfecting the interleukin-3-dependent murine hematopoietic BaF3 cell line with a pGD vector containing *wild-type* (p210 kD) BCR-ABL1 (B2A2) cDNA.[26,61,62] BALB/c 3T3 A31 mouse embryonic fibroblasts (ATCC Cat. CCL-163), expressing PDGFR-A and -B were obtained from B. J. Druker (Oregon Health and Science University, Portland, Oregon). BaF3-Tel-PDGFRβ,28 transduced with a fusion protein comprised of the dimerising portion of TEL and the transmembrane and kinase domain of the PDGFRβ, were provided by D. G. Gilliland (Brigham and Women's Hospital and Harvard Medical School, Boston, Massachusetts). GIST882, a human gastrointestinal stromal tumour (GIST) cell line expressing an activating KIT mutation (exon 13, K642E) was provided by J. Fletcher (MIT Cancer Center and Department of Biology, Cambridge, Massachusetts). MOLM13 were obtained from Yoshinobu Matsuo, Fujisaki cell center, Hayashibara Biochemical Labs Inc. 675-14 Fujisaki, Okayama 702-8006, Japan. MV4-11 were obtained from J. D. Griffin, Dana-Farber Cancer Institute, Boston, Massachusetts.

Cells were cultured in RPMI-1640 (Amimed cat. # 1-14F01-I) supplemented with 2% L-glutamine (Amimed cat. # 5-10K50-H) and 10% FCS (Amimed cat. # 2-01F16-I). *Wild-type*, parental BaF3 cells were maintained in the above medium plus 10 U/mL recombinant mouse IL-3 (Roche # 1380745). The resazurin sodium salt dye reduction assay kit (Alamar Blue™; cat. # DAL1100, BioSource International Inc.) was generally used to measure cell proliferation according to supplier instructions. Briefly, 15000 cells were seeded in 190 µL fresh medium into 96-well plates, followed by addition of 10 µL medium containing compound dilutions at 20-fold their final intended concentration. Cells treated with vehicle (DMSO, 0.1% FCS) only served as controls. Dose-response effects were determined by 3-fold serial dilutions of the test compound, starting at 10 µM. Following incubation of the cells for 48 h at 37°C and 5% CO_2, the effect of inhibitors on cell viability was assessed following addition of 20 µL resazurin sodium salt solution (130 µg/mL PBS) and incubated for an

additional 6 h at 37°C and 5% CO_2. The levels of resorufin,[46] were quantified using a SaphireII 96-well fluorometer (TECAN, Männedorf, Switzerland) with excitation and emission wavelengths set at 544 and 590 nm, respectively. In addition, a plate blank value was determined in a well containing only 100 µL of medium and no cells. Acquired raw data were exported to Excel-file format. For data analysis, the plate blank value was subtracted from all data points. The effect of a particular test compound concentration on cell proliferation and viability was then expressed as percentage of the corrected fluorescence reading obtained for cells treated with vehicle only, which was set as 100%. GI_{50} values were determined using XLfit (V4.2) curve-fitting software, applying standard four parameter logistic model #205 (IDBS, Guilford, UK). The luminescent ATP detection assay kit, ATPLite™ (Perkin Elmer Life Sciences; cat. # 6016947), based upon the production of light (luminescence) caused by the reaction of ATP with added luciferase and D-luciferin, was used to measure the proliferation of GIST882 cells following 70 h incubation with midostaurin according to our published method.[47]

RESULTS

Biochemistry. Kinase inhibition was determined using recombinant enzymes in transphosphorylation assays. Initially the effects of compounds (two determinations in all cases) at a fixed concentration of 10 µM (solubility became limiting at higher concentrations) was assessed against 320 *wild-type* protein kinases and 13 phospatidyl-inositol lipid kinases. In this preliminary screen, midostaurin, **3** and **4** gave residual activity of <50% (n = 2) for 159, 178 and 103 protein kinases respectively (corresponding to selectivity scores at 10 µM of 0.534, 0.575 and 0.347),[12] whereas none of the lipid kinases were substantially inhibited (Table 1).

Table 1: Comparison of the overall selectivity profiles of midostaurin and major metabolites against 94 *wild-type* protein kinases.

Compound	Number of protein kinases inhibited			
	IC_{50} ≤ 10 µM	IC_{50} ≤ 1.0 µM	IC_{50} ≤ 0.1 µM	IC_{50} ≤ 0.01 µM
Midostaurin (**1**)	93	81	22	0

CGP62221 (**3**)	94	75	16	1
4 (e1)	85	24	1	0
4 + **5** (e1 + e2)[1]	86	27	2	0

Based upon the extent of percentage residual phosphorylation activity compared to control in the full panel and the pharmacological importance of the target, dose-response curves were then generated and IC_{50} values determined for midostaurin and the metabolites **3**, **4** (e1) and CGP52421 (a 1:1 mixture of e1 + e2) against 94 *wild-type* enzymes, together with two mutant forms of FLT3 and nine mutant forms of KIT (Tables 1 and 2). In all cases investigated, where the residual activity was >50% in the preliminary screen, the measured IC_{50} value was >5 μM. Most of the *wild-type* kinases showing substantial sensitivity (IC_{50} < 3 μM) to the four compounds were members of the tyrosine kinase (TK) group (40 of 76 evaluated; full complement 90), although at a concentration of 10 μM none of the compounds reduced the residual activity of any of the ephrin TKs by >50%. Many serine-threonine kinases of the AGC (protein kinase A, G and C kinases), CAMK (Ca- and calmodulin-regulated kinases) and STE (homologues of the yeast sterile kinases) families were also potently inhibited, although those of the CMGC (cyclin-dependent kinases, MAP kinases, glycogen synthase kinases, casein kinase 2) and CK1 (casein kinase) groups were insensitive at concentrations < 10 μM.

Table 2: Comparison of the concentrations of midostaurin and major metabolites required to inhibit the transphosphorylation activity of selected protein kinases (IC_{50} values in μM). Kinases are tabulated according to group.[1,2]

Kinase (listed by group)	**Midostaurin**	**3** (CGP62221)	**4** (e1)	**4** + **5** (e1 + e2)[1]
TK: Tyrosine kinase group				
ACK1	0.079	0.143	0.227	0.259
ALK (GST-HIS-tag)	0.645	0.846	2.25	0.879
BLK	0.183	0.576	0.100	0.344
BMX	0.578	0.240	1.37	0.929
BTK	0.669	1.39	2.17	2.60
CSF1R	0.190	0.192	0.523	0.668
CSK	0.708	1.30	1.28	1.38
DDR2	0.566	0.670	0.976	1.72
EGFR	0.687	1.48	1.69	1.43
FER	0.253	0.056	1.78	0.878
FES	0.989	1.01	4.75	2.90

FGFR2	0.225	0.241	1.87	0.554
FLT3 *wild-type*	0.048	0.062	1.19	1.66
FLT3 ITD	0.026	0.024	0.337	0.361
FLT3 D835Y	0.014	0.014	0.186	0.277
FYN	0.263	0.858	0.863	1.24
HCK	0.392	1.54	1.28	1.04
IGF-1R	0.220	0.179	0.154	0.130
INSR	6.32	2.93	7.58	6.48
INSR-R	2.05	1.37	4.47	3.96
JAK2	0.229	0.415	1.80	1.71
JAK3	0.056	0.062	0.459	0.300
KIT *wild-type*	2.17	4.46	3.79	6.23
KIT A829P	0.533	1.38	2.54	2.55
KIT D816H	0.045	0.084	0.229	0.663
KIT D816V	0.066	0.080	0.197	0.615
KIT T670I	0.058	0.115	2.42	2.21
KIT V559D	0.392	0.673	0.920	1.39
KIT V559D / T670I	0.083	0.218	1.66	1.84
KIT V559D / V454A	0.432	1.21	2.15	3.21
KIT V560G	0.101	0.110	0.426	0.392
KIT V654A	1.21	1.23	4.21	4.18
LCK	0.144	2.22	1.09	0.968
LTK	0.180	0.292	2.00	0.307
LYN	0.210	0.810	0.383	0.429
MERTK	1.07	0.691	5.22	4.69
MUSK	0.275	0.330	3.05	2.77
PDGFR-α	0.304	0.335	0.811	1.04
PDGFR-β	0.081	0.107	0.300	0.451
RET	0.026	0.068	0.940	1.39
ROS	0.128	0.044	1.62	3.45
SRC (GST-HIS-tag)	0.469	1.94	2.82	2.07
SYK (aa1-635)	0.194	0.126	1.87	0.983
TNK1	0.074	0.224	1.18	1.56
TRK-A	0.050	0.016	1.20	0.489
TRK-B	0.123	0.047	1.71	0.489
TRK-C	0.055	0.079	1.22	1.43
TYK2	0.357	0.568	3.27	4.53
VEGFR-2	0.015	0.029	0.057	0.062
ZAP70	0.683	0.577	3.02	2.11
AGC: Protein kinase A, G and C family of serine-threonine kinases				
GRK7	0.187	0.080	2.06	2.09
PDPK1	0.078	0.071	0.385	0.097
PKA	0.409	0.896	1.11	1.79
PKC-α	0.220	0.646	4.38	1.53
PKC-β1	0.419	0.944	7.67	2.71
PKC-β2	0.210	0.454	4.60	1.44
PKC-γ	0.225	0.692	3.50	1.07
PKC-δ	0.109	1.49	3.32	1.70
PKC-ε	0.223	2.13	7.95	7.16
PRK1	0.100	0.333	0.908	1.15
PRK2	0.048	0.296	1.56	1.86

PRKG1	0.181	0.214	1.25	1.56
PRKG2	0.018	0.007	0.118	0.174
PRKX	0.878	1.00	6.87	9.13
RPS6KA2	0.051	0.043	1.05	0.969
RPS6KA3 (alias RSK2)	0.070	0.070	0.898	1.04
RPS6KA6	0.033	0.044	0.974	1.02
CAMK: Calcium and calmodulin-regulated group of serine-threonine kinases				
BRSK2	1.66	0.780	> 10	> 10
CAMK2A	0.445	0.820	8.58	6.99
CAMK2D	0.170	0.251	5.18	4.85
CAMK2G	0.681	1.56	8.89	8.90
CAMKK2	0.136	1.08	1.90	1.31
CHK1	1.80	0.261	8.76	2.31
DAPK1	8.60	1.94	> 10	> 10
DAPK3	5.16	1.14	> 10	> 10
MELK	0.563	0.341	9.11	> 10
MYLK	1.18	0.593	6.49	8.50
PHKG1	0.056	0.120	1.23	2.20
PHKG2	2.30	0.315	> 10	> 10
PIM1	0.388	0.281	1.44	1.17
PIM3	0.704	0.294	> 10	4.64
SIK1	0.235	0.675	0.787	1.08
SIK2	0.111	0.125	0.296	0.700
SNRK	0.294	0.598	3.85	5.07
STK17A	1.78	0.914	5.34	7.38
STK33	0.385	0.521	5.60	6.92
STE: Homologues of the yeast sterile kinase family of serine-threonine kinase				
MAP3K7 / MAP3K71P1	0.355	1.31	3.32	2.81
MAP3K9 (alias MLK1)	0.073	0.224	0.527	0.221
MAP3K10	0.063	0.361	0.902	0.425
MAP3K11	0.029	0.195	0.484	0.278
MAP4K2	0.290	0.966	2.84	3.03
MAP4K5	0.470	1.76	> 10	> 10
MST1 (alias STK4)	0.032	0.137	0.648	0.602
MST2	0.256	0.978	2.11	2.48
SLK	0.309	0.959	7.36	6.36
TKL: Tyrosine kinase-like family				
LRRK2	0.102	0.163	4.17	5.11
Other				
AURK-A	0.164	0.247	2.08	3.78
AURK-B	0.247	0.192	0.757	0.992
AURK-C	0.305	0.459	4.65	8.51
GSG2	7.86	0.863	> 10	> 10
IKK-ε	0.100	0.587	1.82	1.07
SAK (alias PLK4)	0.157	0.662	2.27	8.38
TKB1	0.135	0.630	1.63	0.896
TSF1	0.436	0.358	> 10	> 10
WEE1	> 10	1.99	> 10	8.96

[1] Apparent IC_{50} for 1:1 mixture.

Midostaurin, in addition to potently inhibiting *wild-type* FLT3, as well as mutant forms of FLT3 and KIT, inhibited 21 additional kinases with IC_{50} values ≤ 100 nM and a total of 81 *wild-type* kinases with IC_{50} values ≤ 1000 nM. CGP62221 (**3**) showed a similar pattern of selectivity against the 320 protein kinases, as well as similar degrees of potency to that of midostaurin, although it was slightly more potent (≈ 3-fold) against CHK1, FER, PRKG2, ROS, TRK-A / –B, and markedly less active (> 6-fold) against LCK, PKC-δ / -ε, PRK2, CAMKK2 and MAPK11. Both **4** (e1) and e2 maintained potency against VEGFR2 (neither midostaurin nor the metabolites inhibited VEGFR1 by >50% at 10 μM), but in general the presence of a hydroxyl-group in the lactam-ring resulted in reduced activity. Metabolite e1 (**4**) only inhibited 13 kinases with IC_{50} values < 400 nM, all of which were potently inhibited by both midostaurin and CGP62221. In comparison to e1 (**4**), e2 (**5**) was apparently more active (IC_{50} [e1+e2] ≤ 3-fold IC_{50} [e1]) against FGFR2, LTK, TRKB and PDPK1, and clearly much less active (IC_{50} [e1+e2] ≥ 3-fold IC_{50} [e1]) against BLK and the D816 mutant forms of KIT.

Cell proliferation /viability assays

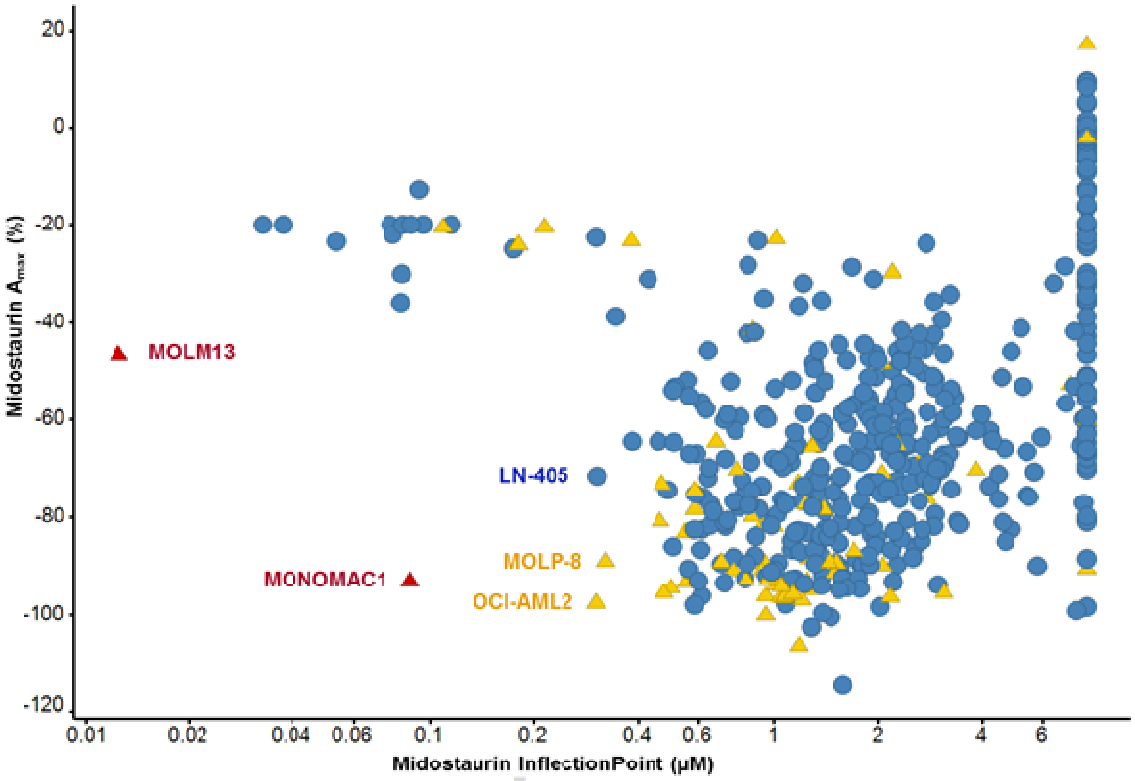

Figure 4. Antiproliferative profile of midostaurin across a large panel of human cancer cell lines. The scatter plot shows the maximun effect level, A_{max} (%), versus inflection point (μM) of midostaurin in cell viability assays assessed on 469 cell lines. Cell lines with A_{max} ≤30% are typically classified as non-responding. Cells carrying mutated FLT3 (MOLM13 and MONOMAC1) are depicted as red triangles, with 65 other hematopoietic cell lines depicted as yellow triangles and solid tumor cell lines as blue circles.

Although midostaurin impacted the viability of many cell lines in the CCLE screen at concentrations > 400 nM (Figure 4), it showed considerable selectivity at lower concentrations (A_{max} levels < 30% were not regarded as being of significance). The greatest activity was seen towards the human AML cell lines MOLM13 and MONOMAC1, the viability of which was substantially curtailed at concentrations ≤ 100 nM (due to the curve fitting algorithm employed the MOLM13 A_{max} is underestimated and should be ≈70%; Supplemental Figure S1). The proliferation of OCI-AML2 AML, MOLP-8 multiple myeloma

and LN-405 glioma cell lines were also substantially impacted at concentrations in the range of 300-400 nM.

Table 3: Comparison of the effects of midostaurin, CGP62221 and [**4** + **5**] (the CGP524211:1 mixture of e1 and e2) on cell lines dependent and independent upon midostaurin-sensitive (IC_{50} < 500 nM; no fill) and –insensitive kinases (grey fill) and untransduced BaF3 cells (mean GI_{50} nM ± SEM; n ≥ 3).

Kinase	Cell line	Effect on cell proliferation [1]		
		Midostaurin	CGP62221 (3)	4 + 5
FLT3-ITD	BaF3-FLT3-ITD	39 ± 2	28 ± 6	656 ± 155
FLT3-ITD	MOLM13 (heterozygous)	48.4 ± 6.9	n.d. [2]	n.d.
FLT3-ITD	MV4-11 (homozygous)	26.3 ± 7.1	n.d.	n.d.
IGF-1R	BaF3-Tel-IGF-1R	319 ± 38	189 ± 31	1315 ± 269
KIT (D816V)	BaF3-KIT-D816V	88 ± 6	50 ± 7	319 ± 28
PDGFRβ	BaF3-Tel-PDGFRβ	19 ± 3	< 12 [3]	63 ± 9
RET	BaF3-PTC3-RET	96 ± 7	167 ± 27	1216 ± 180
ABL1 [4]	BaF3-BCR-ABL1	655 ± 91	1218 ± 85	> 10000
ALK	BaF3-NPM-ALK	364 ± 8	196 ± 54	2316 ± 630
FGFR3	BaF3-Tel-FGFR3	373 ± 41	497 ± 82	5071 ± 323
INSR	BaF3-Tel-INSR	253 ± 25	152 ± 15	1046 ± 201
KIT (K642E)	GIST882	399 ± 171 [5]	n.d.	n.d.
Untransduced BaF3 *wild-type*		388 ± 11	327 ± 89	3657 ± 459

[1] The Alamar Blue™ assay was used for all cell lines with the exception of GIST882, where the ATPLite™ assay was employed (see Experimental section for details); [2] n.d.: not determined; [3] three determinations gave IC_{50} values of 12, < 5 and < 5 nM; [4] none of the compounds reduced the residual transphosphorylation activity of ABL1 by >35% at 10 μM; [5] midostaurin inhibited K642E KIT autophosphorylation with an IC_{50} value of 4523 ± 1805 (n=5) in GIST882 cells as determined by capture ELISA[48] (J. Mestan, unpublished results).

The effects of compounds on cell viability was further tested on a small panel of human cancer cells and engineered murine hematopoietic cell lines. Murine interleukin (IL)-3-dependent pro-B lymphoma cells (*wild-type* BaF3) were used to generate sub-lines whose proliferation and survival was rendered IL-3 independent by stable transduction with individual tyrosine kinases either activated by mutation or fusion with a dimerizing protein partner.[45,48] The effects of compounds on cell viability were generally assessed using the resazurin assay in which viable cells reduce resazurin to the highly fluorescent resorufin, whereas non-viable cells rapidly lose their reductive capacity and fail to produce a fluorescent signal,[46] although in the case of GIST882 the ATPLite™ assay was employed to measure ATP concentrations

which rapidly decline when cells undergo necrosis or apoptosis.[47] The effects on cell viability are compared in Table 3. In general, biochemical kinase inhibition translated into antiproliferative activity. Midostaurin and CGP62221 (**3**) potently inhibited (GI_{50} < 100 nM) the proliferation of those cell lines driven by FLT3, D816V KIT, PDGFRβ and RET. However both compounds, also inhibited the viability of *wild-type* BaF3 cells (GI_{50} 300-400 nM), and midostaurin in particular reduced the viability of BaF3-BCR-ABL1, BaF3-Tel-INSR and human gastrointestinal stromal GIST882 cells. In contrast, the epimeric mixture of metabolites [e1+e2] substantially inhibited the proliferation of only the Tel-PDGFRβ (GI_{50} 63 nM), D816V KIT (GI_{50} 320 nM) and FLT3-ITD (GI_{50} 650 nM) BaF3 cell lines, while the *wild-type* cells were relatively insensitive.

DISCUSSION

Collectively AML is the most common form of adult leukemia, having an incidence of 4.2 per 100,000 population with an overall 5-year survival rate of 27% in the U.S.A. in the period 2007-2013.[49] However, AML is a heterogeneous malignancy that arises from hematopoietic progenitor cells which progressively acquire large, diverse sets of coexisting cytogenetic and epigenetic lesions leading to the activation of pro-proliferative pathways and impaired normal hematopoietic differentiation.[50,51] Consequently, as suitable targeted therapies become available, different AML genotypes should mandate different therapeutic interventions.[37] Gain-of-function mutations in the FLT3 gene are detected in about 30% of AML patients, with the majority (≈ 66%) of these being ITD mutations that confer an adverse prognosis compared to FLT3 kinase domain mutations, or mutations in other genes. Consequently, much hope has been engendered that inhibiting aberrant FLT3 signalling in leukemic cells will provide therapeutic benefit to some groups of AML patients. However, assessing the potential for kinase inhibitors that target FLT3 was confounded in early clinical trials, because the different drugs investigated (Figure 2) had very different target profiles which made

attributing therapeutic effects to biochemical mechanisms problematic.[35] Midostaurin (Rydapt®) has been developed as an FLT3 inhibitor and is the first targeted therapy to receive Health Authority approval for the treatment of AML,[31] but as presented here its efficacy is probably the result of a complex interplay between the kinase activities of the drug and its metabolites.

In order to compare the kinase profiles of midostaurin with that of the three major metabolites, in addition to CGP62221 (**3**) which was readily prepared by benzoylation of the methylamine precursor available from the fermentation broth of a mutant strain of Streptomyces longisporoflavus,[40] it was necessary to have a discrete sample of at least one of the two epimers of the CGP52421 mixture (Figure 1). Using the method of Kasai and co-workers,[52] oxidation of **1** with DDQ afforded a 1:1 mixture of the two epimeric C3-hydroxylated derivatives, e1 and e2, as detected in midostaurin-treated patients. Whereas the more lipophilic epimer, e1 was sufficiently soluble to be purified by column chromatography, epimer e2 defied attempts at purification and, when dissolved in protic solvents, such as methanol afforded an epimeric mixture of 3-methoxy derivatives. Single-crystal X-ray diffraction studies of e1 showed it to correspond to **4**, having (3*S*,9*S*,10*R*,11*R*,13*R*) absolute stereochemistry, thus inferring that e2 had (*R*)-stereochemistry at the corresponding 3-position of **5**. The instability of **5** is analogous to that reported for the hydroxylated staurosporine,[53] UCN-01 (Figure 2) and such epimerisations probably stem from the ease of formation of an intermediate 1H-isoindolin-1-one.[54-56] Liquid chromatography - mass spectroscopy studies unambiguously confirmed that **4** corresponds to epimer e1, thus allowing *in vitro* characterization of the metabolites.

Weisberg and coworkers[29] first reported that midostaurin and the epimeric 1:1 mixture of metabolites [e1 + e2] (CGP52421), inhibited the transphosphorylation activity of recombinant GST-FLT3 in a radiometric assay (8 μM ATP; substrate: poly{GluTyr}4:1) with IC_{50} values

of 528 and 643 nM respectively. Without invoking intracellular drug accumulation, this relatively weak activity was inconsistent with their findings in murine BaF3 cells transfected to express either ITD- or D835Y-mutant FLT, where midostaurin abbrogated FLT3 autophosphorylation at concentrations substantially below 1 μM. The BaF3 results were subsequently supported by studies employing FTL3-dependent human leukemia cell lines, where midostaurin potently inhibited the autophosphorylation of *wild-type* (RS4;11 cells) and ITD FLT3 (MV4-11 cells) with IC_{50} values of 15 and 13 nM respectively.[57] This autophosphorylation data is consistent with results from the present biochemical study, where midostaurin potently inhibited the transphosphorylation activity of the *wild-type*, as well as the ITD- and D835Y-mutant forms of FLT3 with IC_{50} values of 48, 26 and 14 nM respectively, and was further corroborated using the InVitrogen SelectScreen™,[58] where the drug inhibited *wild-type* and D835Y FLT3 with IC_{50} values of 20 and 3.6 nM respectively. Here we show that the major metabolites also inhibit the kinase activity of FLT3, with CGP62221 (**3**) possessing activities comparable to those of the parent drug, while e1 (**4**) and e2 (**5**) have IC_{50} values in the range of 200-400 nM against the ITD and D835Y mutants, and low micromolar activity against the *wild-type* enzyme. However, when taking into consideration that following chronic dosing, steady-state plasma trough levels of CGP62221 (**3**) are slightly higher than those of midostaurin and those of e2 (**5**) are about 8-fold higher, it is expected both metabolites make important contributions to the inhibition of FLT3-catalysed phosphorylation in the leukemic cells of AML patients.

In addition to targeting FLT3, together with kinases such as those of the PKC family and VEGFR2 which had supported the initial clinical development of midostaurin,[15,31] here we show that midosaurin inhibits a large number of additional tyrosine and serine-threonine kinases, with IC_{50} values substantially below 1 μM. The major metabolite CGP62221 (**3**) is also a multitargeted-kinase inhibitor, possessing a similar potency and selectivity profile to that of midostaurin, although the 4-fold greater inhibition of FER is perhaps of significance.

The activities of midostaurin and CGP62221 against the mutant forms of KIT are of particular relevance since in addition to being involved in SM,[5] a high expression level of this proto-oncogene is a poor prognostic marker in AML and activating KIT mutations, which mainly occur in the activation loop of the kinase domain (exon 17) resulting in Asp816Val and Asn822Lys substitutions, are found in 25 - 30% of cases of core-binding factor (CBF)-AML.[59,60]

In contrast to CGP62221 (**3**), the 3-hydroxylated metabolites **4** and **5** are generally less active and have somewhat different selectivity profiles, resulting in an increased selectivity towards VEGFR2. Since **4** is only a minor metabolite, given its kinase profile it is unlikely to play a substantial contribution to the pharmacology of midostaurin in patients. However, because **5** accumulates to become the major circulating component, the kinase targets of this metabolite, and PDPK1 in particular, considering that it is over-expressed in AML and promotes PKC-mediated survival of leukemic blasts,[61,62] are likely to contribute to the pharmacology of the parent drug.

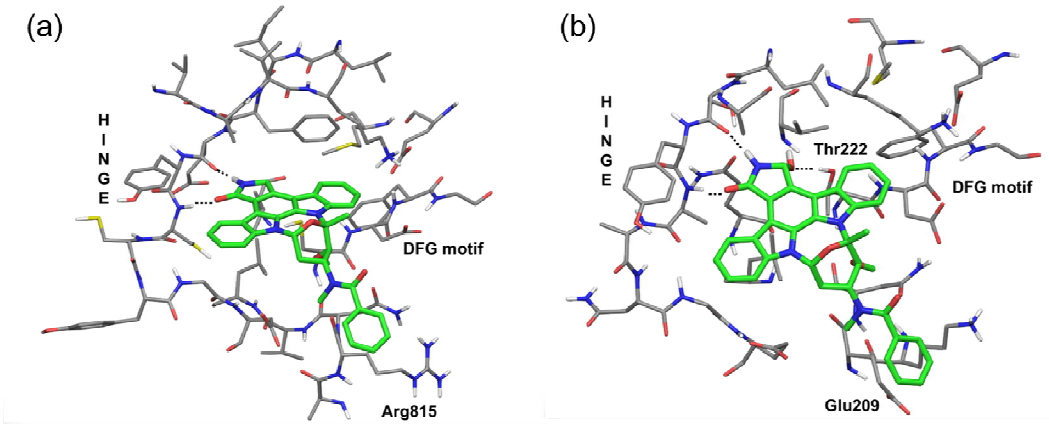

Figure 5. Representations of (**a**) midostaurin docked into a homology model of an active conformation of FLT3 (based upon the staurosporine-LCK cocrystal structure;[65] pdb# 1QPJ) and (**b**) epimer e2 (**5**) docked into PDPK1 (based upon the UCN-01 - PDPK1 cocrystal structure; [64] pdb# 1OKZ). The carbon atoms of ligands and kinases are depicted in green and

grey respectively, with nitrogens, oxygens and sulphurs shown in blue, red and yellow respectively; H-bonds are depicted as dotted black lines. The lactam moieties of both ligands make bidentate H-bond interactions with backbone amides of the hinge region of the kinase SH1 domains, mimicking the amidine group of ATP. The selectivity of midostaurin over staurosporine can be attributed to (i) the absence of a basic MeNH-group capable of interacting with acidic residues (*e.g.* Glu91 in CHK1) in the ribose-pocket,[64] and (ii) the bulky benzoyl group impeding binding, except to kinases where it can make favourable hydrophobic contacts with the hydrocarbon part of the side-chains of adjacent residues: FLT3 (Arg815), JAK3 (Arg953), RET (Arg624), VEGFR2 (Arg1030) and PDPK1 (Glu209; analogous to that with Glu291 reported between midostaurin and DYRK1A.[62] Although **4** and **5** are generally a much less potent kinase inhibitors, **5** maintains activity against PDPK1, which is attributable to the 3-*R*-hydroxy group H-bonding to Thr222, analogous to that observed with UCN-01.

Although co-crystallization studies with midostaurin are impeded by the poor solubility of the ligand, modelling studies based upon the only available co-crystal structure with DYRK1A,[63] can in part explain the observed kinase selectivities (Figure 5). In general, the 3-hydroxy groups of **4** and **5** lead to reduced kinase activity due to the lack of favorable interactions to overcome desolvation, although the potent inhibition of PDPK1 by **5** can be rationalised by an interaction between the 3-*R*-hydroxy group and the side-chain hydroxyl of the Thr222 residue (DFG-1), analogous to that observed with the hydroxystaurosporine UCN-01.[64] However, unlike UCN-01 which also potently inhibits CHK1, the benzoyl groups of midostaurin and its metabolites make electrostatically and sterically unfavorable contact with the Glu91 residue of this kinase.

To investigate the effects of inhibiting many kinases in cells, midostaurin was profiled against a large panel of human cancer cell lines in the CCLE. The drug showed greatest

antiproliferative activity against the MOLM13 and MONOMAC1 AML cells which harbour ITD and V592A FLT3 mutations respectively.[66,67] It also substantially reduced the viability of the OCI-AML2 AML and the MOLP-8 multiple myeloma cell lines. The effect on OCI-AML2 cells (Supplementary Figure S1) is notable since these cells carry a point mutation in the *DNMT3A* gene, which encodes an R635W amino-acid replacement in the DNA methyltransferase domain, and *DNMT3A* is frequently mutated in AML patients and is associated with a poor outcome.[51,68-70] Also of possible relevance is the activity against the MOLP-8 cell-line (Supplementary Figure S2), the genotype of which shows loss of *CDKN2A* (a tumor suppressor gene), loss of *PTEN*, together with a gain-of-function mutation in *NRAS*. However, at present it is not known which target(s) of midostaurin underlie the antiproliferative effects of the drug in these two cell lines.

Further insight into the cellular activity of the compounds against non-FLT3-dependent cells comes from a comparison of their effects on a panel of cells derived from either human tumors or murine hematopoietic BaF3 cells rendered growth-factor independent by transfection with constructs encoding constitutively active protein kinases (Table 3). The inhibition of FLT3-ITD kinase biochemical activity translated into potent antiproliferative activity in FLT3-ITD dependent BaF3, MOLM13 and MV4-11 cells, with potencies comparable with those reported to inhibit the phosporylation of FLT3 and its signalling in a variety of FLT3-dependent AML cells.[29,71,72] As expected, potent activity leading to a high degree of selectivity was also evident towards those cells dependent upon other kinases that were strongly inhibited in the biochemical screen (D816V KIT, PDGFRβ and RET). However, unlike **4** and **5** [e1+e2], both midostaurin and CGP62221 (**3**) also inhibited the proliferation of *wild-type* BaF3 cells (GI_{50} values 388 and 327 nM respectively), and midostaurin in particular reduced the viability of BaF3-BCR-ABL1 (GI_{50} 655 nM), BaF3-Tel-INSR (GI_{50} 253 nM) and human gastrointestinal stromal GIST882 cells (GI_{50} 399 nM) that are dependent upon constitutively activated kinases not targeted by the drug (ABL1, INSR

and K642E KIT). This pattern of activity is consistent with midostaurin and CGP62221 inhibiting one or more elements of the IL-3 signalling pathway in *wild-type* BaF3 cells and elements downstream of the oncogenic kinases that drive the proliferation of the other cell lines.

An effect on the IL-3 signalling pathway is potentially of particular relevance to the treatment of AML, since IL-3 regulates the production of hematopoietic cells and overexpression of the IL-3 receptor α-chain has been shown to provide a survival and growth advantage to leukemic cells, and is associated with poor prognosis.[73] However, as for the OCI-AML2 and the MOLP-8 cells, deconvoluting the kinase target(s) responsible for inhibiting downstream signalling and causing the general cytotoxicity seen in the CCLE screen at concentrations of ≥4 μM is not straightforward. Several protein kinases have been reported to be elements in multiple IL-3 signal transduction pathways, including JAK-, MAPK- and SRC-family kinases,[74] and a number of kinases (AURK-A, CAMK2D, FLT3, GRK7, LRRK2, PHKG1, PRKG2, RET, ROS, RPS6KA, TRK-A, TYK2) are shown in this study to be potently inhibited by midostaurin and CGP62221 with IC_{50} values <300 nM, while remaining relatively insensitive (≥10-fold less active) to **4** and **5** (Table 2). In addition to FLT3 and KIT, a number of other kinases including several of those mentioned above, have been implicated in playing a role in various genotypes of AML, either as elements of signaling pathways in AML cells or implicated by providing stromal support (Table 4). Several of these are substantially inhibited by midostaurin and its metabolites at physiologically relevant concentrations and consequently activity against these targets probably contributes to the pharmacological effects of the drug in AML patients carrying FLT3 mutations.

Table 4: Kinases other than FLT3 or KIT that have been implicated as playing a role in AML and their sensitivity towards midostaurin and metabolites.

Kinase	Role	Sensitivity[1]
AKT / PI3K	FLT3-ITD in AML is associated with activation	Insensitive

families	of the PI3K/AKT pathway.[75]	
AURK-A / -B	Regulate mitosis; inhibitors reduce viability of AML cells and have shown efficacy in patients.[76,77]	100 – 300
AXL	Overexpressed in AML and associated with resistance to FLT3 inhibitors.[78,79]	Insensitive
CHK1	Mediates AML cell proliferation downstream of ITD-FLT3.[80]	200 – 300
FES	Downstream signalling element of ITD-FLT3 in AML cells,[81] and of D816V in neoplastic mast cells.[5]	Insensitive
HCK	Required for proliferation of AML cells, controls CDK6 expression and overexpressed in LSCs.[82]	Insensitive
IGF1R	IGF-1 autocriny plays a role in primary AML cells.[83,84]	100 – 300
JAK family	JAK kinases regulate STAT3, the activity of which is frequently increased in AML.[74,85]	50 – 300
LYN / SRC family	LYN major active SRC family member expressed in AML cells.[74,86-88]	200 - 300
PDPK1	Master kinase overexpressed in AML cells, promotes survival of blasts and associated with poor outcome.[61,62]	<100
PIM-1	Overexpressed in AML cell which are highly sensitive to PIM inhibition; mediates FLT-3 inhibitor resistance.[89-91]	200 – 300
PLK1	Overexpressed in AML; volasertib (inhibition (volasertib) shows some efficacy in AML.[92]	Insensitive
RET	MLL-AFP AML cells dependent upon RET expression;[93] RET-mTOR signaling promotes AML through protection of FLT3-ITD mutants from autophagic degradation.[94]	<100
SYK	FLT3-ITD AML cells are sensitive to SYK suppression.[95]	100 – 200
TRKA	Overexpressed in AML and activating mutation detected in patients and targeted by lestauritinib.[96]	<100
VEGFR	AML bone marrow highly vascularised and AML cells secrete VEGF and express VEGFRs.[97]	<100

[1] IC_{50} range (nM). Kinases are considered to be sensitive to midostaurin, CGP62221 or [e1+e2] when $IC_{50} < 300$ nM.

This notion finds some circumstantial support in the emergence of midostaurin resistance: A liability of cancer therapies targeting oncogenic tyrosine kinases is the emergence of drug resistance leading to patient relapse.[98-101] This is best exemplified by secondary resistance to imatinib in chronic myeloid leukemia patients which is frequently the result of mutant clones emerging that harbor amino-acid substitutions in the kinase domain of BCR-ABL1 that either directly impede drug binding or destabilise the inactive conformational of the oncogenic kinase to which the drug binds.[98,101] Such reactivation of a kinase signalling pathway through mutations can therefore provide supportive evidence for the mechanism of action of the

targeting drug. The emergence of kinase inhibitor resistance can be recapitulated *in vitro* by a variety of methods,[102] and several such studies have been performed with FLT3 inhibitors that have been investigated in AML patients. Thus on incubating randomly mutated ITD-FLT3 transformed BaF3 cells with midostaurin, it was discovered that substitutions of Asn676, Gly697 and Phe691 (the most frequently detected Phe691Leu "gate-keeper" mutation remained sensitive) could confer resistance.[103-105] However, upon prolonged incubation of human leukemic cell lines (MOLM or MV4-11) with sublethal concentrations of midostaurin none of the resistant clones that emerged expressed secondary FLT3 kinase mutations.[106,107] Furthermore there is only one report of the emergence of midostaurin resistance in a patient resulting from a secondary mutation in ITD-FLT3 (Asn676Lys).[108] In contrast resistance is conferred to the investigational AML drug quizartinib (Figure 2) by Asn676, Phe691, Gly697, Asp835 and Tyr842 FLT3 kinase domain substitutions in ITD-FLT3 BaF3 cells,[105,109,110] and of eight ITD-FLT3 AML patients who relapsed to quizartinib all harbored Asp836 or Phe691 mutations.[109] Quizartinib is a type-2 ATP-competitive kinase inhibitor,[38] which selectively inhibits several receptor TKs (FLT3, CSF1R, KIT, PDGFR and RET)[57,111] and as a consequence, unlike midostaurin it does not have the capability to effect cytosolic kinases that mediate downstream signaling from FLT3 or other pathways that might be involved in supporting the AML phenotype.

In summary, through extensive kinase profiling we have shown that like midostaurin, the major metabolites CGP62221 (**3**) and **5** possess protein kinase inhibitory activities that probably contribute to the efficacy of midostaurin as a drug in the treatment of AML and engender the distinctive effects of midostaurin compared to other FLT3 inhibitors in this malignancy.

ASSOCIATED CONTENT

Supporting Information. The concentrations of ATP, enzymes and substrates employed are for the biochemical studies are provided in Supplementary Table 1. Crystallographic data (excluding structure factors) have been deposited with the Cambridge Crystallographic Data Centre as supplementary publication number CCDC ######. Copies of the data can be obtained free of charge on application to CCDC, 12 Union Road, Cambridge CB2 1EZ, UK [fax (+44) 1223 336033, email: deposit@ccdc.cam.ac.uk]. This material is available free of charge via the internet at http://pubs.acs.org.

Supplementary Figure S1

Supplementary Table S1

ACKNOWLEDGEMENTS

We gratefully acknowledge Drs. J. D. Griffin (Dana-Farber Cancer Institute, Boston, USA) and D. G. Gilliland (Brigham and Women's Hospital and Harvard Medical School, Boston, USA) for their collaboration in generating the BaF3 cell lines used in this study. All of the authors of this manuscript were full-time employees of Novartis Pharmaceuticals when they carried out their work and no external funding sources, grants or awards were used to generate the any of the reported fnidings.

Authorship Contributions

P.W.M. designed and commissioned studies, and wrote the manuscript. P.W.M., G.C., J.R,. P.T, T.W. and M.W. performed/oversaw experiments. J.R., P.F., P.T., T.W. and M.W. contributed to data analysis.

REFERENCES

[1] Manning, G., Whyte D. B., Martinez. R., Hunter, T., and Sudarsanam, S. (2002) The protein kinase complement of the human genome. *Science 298*, 1912-1934.

[2] Hanks, S. K. (2003) Genomic analysis of the eukaryotic protein kinase superfamily: a perspective. *Genome Biol. 4*, 111.

[3] Stone, R. M., Mandrekar, S. J., Sanford, B.L., Laumann, K., Geyer, S., Bloomfield, C.D., Thiede, C., Prior, T.W., Dohner, K., Marcucci, G., Lo-Coco, F., Klisovic, R. B., Wei, A., Sierra, J., Sanz, M.A., Brandwein, J.M., de Witte, T., Niederwieser, D., Appelbaum, F.R., Medeiros, B.C., Tallman, M. S., Krauter, J., Schlenk, R.F., Ganser, A., Serve, H., Ehninger, G., Amadori, S., Larson, R.A., and Döhner. H. (2017) The multi-kinase inhibitor midostaurin (M) prolongs survival compared with placebo (P) in combination with daunorubicin (D)/cytarabine (C) induction (ind), high-dose C consolidation (consol), and as maintenance (maint) therapy in newly diagnosed acute myeloid leukemia (AML) patients (pts) age 18–60 with FLT3 mutations (muts): An international prospective randomized (rand) P-controlled double-blind trial (CALGB 10603/RATIFY [Alliance]). *N. Engl. J. Med. 377*, 454-464.

[4] Gotlib, J., Kluin-Nelemans, H. C., George, T. I., Akim, C., Sotlar, K., Hermine, O., Awan, F. T., Hexner, E., Mauro, M. J., Sternberg, D. W., Villeneuve, M., Labed, A. H., Stanek, E. K., Hartmann, K., Horny, H., Valent, P., and Reiter, A. (2016) Efficacy and Safety of Midostaurin in Advanced Systemic Mastocytosis. *N. Engl. J. Med. 374*, 2530-2541.

[5] Peter, B., Winter, G. E., Blatt, K., Bennett, K. L., Stefanzl, G., Rix, U., Eisenwort, G., Hadzijusufovic, E., Gridling, M., Dutreix, C., Hoermann, G, Schwaab, J., Radia, D., Roesel, J., Manley, P. W., Reiter, A., Superti-Furga, G., and Valent, P. (2016) Target interaction profiling of midostaurin and its metabolites in neoplastic mast cells predicts distinct effects on activation and growth. *Leukemia 30*, 464-472.

[6] Furusaki, A., Hashiba, N., Matsumoto, T., Hirano, A., Iwai, Y., and Omura, S. (1978) X-ray structure of staurosporine: a new alkaloid from a Streptomyces strain. *J. C. S. Chem. Commun*. *18*, 800-801.

[7] Funato, N., Takayanagi, H., Konda, Y., Toda, Y., Harigaya, Y., Iwai, Y., and Omura, S. (1994) Absolute configuration of staurosporine by x-ray analysis. *Tetrahedron Lett*. *35*, 1251-1254.

[8] Casnellie, J. E. (1991) Protein kinase inhibitors: probes for the functions of protein phosphorylation. *Adv. Pharmacol*. *22*, 167-205.

[9] Fährmann, M. (2008) Targeting protein kinase C (PKC) in physiology and cancer of the gastric cell system. *Current Med. Chem*. *15*, 1175-1191.

[10] Tamaoki, T., Nomoto, H., Takahashi, I., Kato, Y., Morimoto, M., and Tomita, F. (1986) Staurosporine, a potent inhibitor of phospholipid/Ca++dependent protein kinase. *Biochem. Biophys. Res. Comm. 135*, 397-402.

[11] Rüegg, U. T., and Burgess, G. M. (1989) Staurosporine, K-252 and UCN-01: potent but nonspecific inhibitors of protein kinases. *Trends Pharm. Sci. 10*, 218-220.

[12] Karaman, M. W., Herrgard, S., Treiber, D. K., Gallant, P., Corey Atteridge, C. E., Campbell, B. T., Chan, K. W., Ciceri, P., Davis, M. I., Edeen, P. T., Faraoni, R., Floyd, M., Hunt, J. P., Lockhart, D.J., Milanov, Z. V., Morrison, M. J., Pallares, G., Patel, H. K., Pritchard, S., Wodicka, L. M., and Zarrinkar, P.P. (2008) A quantitative analysis of kinase inhibitor selectivity. *Nat. Biotechnol*. *26*, 127-132.

[13] Mochly-Rosen, D., Das, K., and Grimes, K. V. (2012) Protein kinase C, an elusive therapeutic target? *Nature Rev. Drug Discovery 11*, 937-957.

[14] Caravatti, G., Meyer, T., Fredenhagen, A., Trinks, U., Mett, H., and Fabbro, D. (1994) Inhibitory activity and selectivity of staurosporine derivatives towards protein kinase C. *Bioorg. Med. Chem. Lett. 4*, 399-404.

[15] Fabbro, D., Buchdunger, E., Wood, J., Mestan, J., Hofmann, F., Ferrari, S., Mett, H., O'Reilly, T., and Meyer, T. (1999) Inhibitors of protein kinases: CGP 41251, a protein kinase inhibitor with potential as an anticancer agent. *Pharmacol. Ther. 82*, 293-301.

[16] Seo, M. S., Kwak, N., Ozaki, H., Yamada, H., Okamoto, N., Yamada, E., Fabbro, D., Hofmann, F., Wood, J. M., and Campochiaro, P. A. (1999) Dramatic inhibition of retinal and choroidal neovascularization by oral administration of a kinase inhibitor. *Am. J. Pathol. 154*, 1743-1753.

[17] Propper, D. J., McDonald, A. C., Man, A., Thavasu, P., Balkwill, F., Braybrooke, J. P., Caponigro, F., Graf, P., Dutreix, C., Blackie, R., Kaye, S. B., Ganesan, T. S., Talbot, D. C., Harris, A. L, and Twelves, C. (2001) Phase I and pharmacokinetic study of PKC412, an inhibitor of protein kinase C. *J. Clin. Oncol. 19,* 1485-1492.

[18] Campochiaro, P. A. (2004) Reduction of diabetic macular edema by oral administration of the kinase inhibitor PKC412. *Invest. Ophthalmol. Vis. Sci. 45,* 922-931.

[19] Nakao, M., Yokota, S., Iwai, T., Kaneko, H., Horiike, S., Kashima, K., Sonoda, Y., Fujimoto, T., and Misawa, S. (1996) Internal tandem duplication of the flt3 gene found in acute myeloid leukemia. *Leukemia 10*, 1911-1918.

[20] Yokota, S., Kiyoi, H., Nakao, M., Iwai, T.; Misawa, S., Okuda, T., Sonoda, Y., Abe, T., Kahsima, K., Matsuo, Y., and Naoe T. (1997) Internal tandem duplication of the FLT3 gene is preferentially seen in acute myeloid leukemia and myelodysplastic syndrome among various hematological malignancies. A study on a large series of patients and cell lines. *Leukemia 11*, 1605-1609.

[21] Yamamoto, Y., Kiyoi, H., Nakano, Y., Suzuki. R., Kodera, Y., Miyawaki, S., Asou, N., Kuriyama, K., Yagasaki, F., Shimazaki, C., Akiyama, H., Saito, K., Nishimura, M., Motoji, T., Shinagawa, K., Takeshita, A., Saito, H., Ueda, R., Ohno, R., and Naoe T. (2001) Activating mutation of D835 within the activation loop of FLT3 in human hematologic malignancies. *Blood 97*, 2434-2439.

[21] Stirewalt, D. L., and Radich, J. P. (2003) The role of FLT3 in hematopoeitic malignancies. *Nat. Rev. Cancer 3*, 650-665.

[22] Whitman, S. P., Archer, K. J., Feng, L., Baldus, C., Becknell, B., Carlson, B. D., Carroll, A. J., Mrozek, K., Vardiman, J. W., George, S. L., Kolitz, J. E., Larson, R. A., Bloomfield, C. D., and Caligiuri, M. A. (2001) Absence of the wild-type allele predicts poor prognosis in adult de novo acute myeloid leukemia with normal cytogenetics and the internal tandem duplication of FLT3: a cancer and leukemia group B study. *Cancer Res. 61,* 7233–7239.

[23] Thiede, C., Steudel, C., Mohr, B., Schaich, M., Schäkel, U., Platzbecker, U., Wermke, M., Bornhäuser, M., Ritter, M., Neubauer, A., Ehninger, G., and Illmer, T. (2002) Analysis of FLT3-activating mutations in 979 patients with acute myelogenous leukemia: association with FAB subtypes and identification of subgroups with poor prognosis. *Blood. 99*, 4326–4335.

[24] Takahashi, S. (2011) Downstream molecular pathways of FLT3 in the pathogenesis of acute myeloid leukemia: biology and therapeutic implications . *J. Hematol. Oncol. 4*, 13.

[25] Griffith, J., Black, J., Faerman, C., Swenson, L., Wynn, M., Lu, F., Lippke, J., and Saxena, K. (2004) The structural basis for autoinhibition of FLT3 by the juxtamembrane domain. *Mol. Cell 13*, 169-178.

[26] Smith, C. C., Lin, K., Stecula, A., Sali, A., and Shah, N. P. (2015) FLT3 D835 mutations confer differential resistance to type II FLT3 inhibitors. *Leukemia 29*, 2390-2392.

[27] Zhao, M., Kiyoi, H., Yamamoto, Y., Ito, M., Towatari, M., Omura, S., Kitamura, T., Ueda, R., Saito, H., and Naoe, T. (2000) In vivo treatment of mutant FLT3-transformed murine leukemia with a tyrosine kinase inhibitor. *Leukemia 14*, 374-378.

[28] Schenone, S., Brullo, C., and Botta, M. (2008) Small molecules ATP-competitive inhibitors of FLT3: a chemical overview. *Current Med. Chem. 15*, 3113-3132.

[29] Weisberg, E., Boulton, C., Kelly, L. M., Manley, P., Fabbro, D., Meyer, T., Gilliland, D. G., and Griffin, J. D. (2002) Inhibition of mutant FLT3 receptors in leukemia cells by the small molecule tyrosine kinase inhibitor PKC412. *Cancer Cell 1*, 433-443.

[30] Fischer, T., Stone, R. M., DeAngelo, D. J., Galinsky, I., Estey, E., Lanza, C., Fox, E., Ehninger, G., Feldman, E. J., Schiller, G. J., Klimek, V. M., Nimer, S. D., Gilliland, D. G., Dutreix, C., Huntsman-Labed, A., Virkus, J., and Giles, F. J. (2010) Phase IIB trial of oral midostaurin (PKC412), the FMS-like tyrosine kinase 3 receptor (FLT3) and multi-targeted kinase inhibitor, in patients with acute myeloid leukemia and high-risk myelodysplastic syndrome with either wild-type or mutated FLT3. *J. Clin. Oncol. 28*, 4339-4345.

[31] Stone, R. M., Manley, P. W., Larson, R. A., and Capdeville, R. (2018) Midostaurin: Its Odyssey From Discovery to Approval for Treating Acute Myeloid Leukemia and Advanced Systemic Mastocytosis. *Blood Advances 2*, 444-453.

[32] He, H., Tran, P., Gu, H., Tedesco, V., Zhang, J., Lin, W., Gatlik, E., Klein, K., and Heimbach, T. (2017) Midostaurin, a Novel Protein Kinase Inhibitor for the Treatment of Acute Myelogenous Leukemia: Insights from Human Absorption, Metabolism, and Excretion Studies of a BDDCS II *Drug Drug Metab. Dispos. 45*, 540-555.

[33] Wang, Y., Yin, O. Q. P., Graf, P., Kisicki, J. C., and Schran, H. (2008) Dose- and time-dependent pharmacokinetics of midostaurin in patients with diabetes mellitus. *J. Clin. Pharmacol. 48*, 763-775.

[34] Illmer, T., Thiede, H. M., Thiede, C., Bornhaeuser, M., Schaich, M., Schleyer, E., and Ehninger, G. (2007) A highly sensitive method for the detection of PKC412 (CGP41251) and its metabolites by high-performance liquid chromatography. *J Pharmacol. Toxicol. Methods 56*, 23-27.

[35] Stone, R. M. (2017) 3 + 7 + FLT3 inhibitors: 1 + 1 ≠ 2. *Blood 129*, 1061-1062.

[36] Stahl, M., Lu, B. Y; Kim, T. K., and Zeidan, A. M. (2017) Novel Therapies for Acute Myeloid Leukemia: Are We Finally Breaking the Deadlock? *Targ. Oncol. 12*, 413-447.

[37] Sweet, K., and Lancet, J. (2017) State of the Art Update and Next Questions: Acute Myeloid Leukemia. *Clin. Lymphoma Myeloma Leuk. 17*, 703-709.

[38] Liu, Y., and Gray, N. S. (2006) Rational design of inhibitors that bind to inactive kinase conformations. *Nat. Chem. Biol. 2,* 358-364.

[39] Hoehn, P., Koch, B., Mutz, M. Crystalline forms of benzoylstaurosporine. Patent WO 2006048296, 2005.

[40] Hoehn, P., Ghisalba, O., Moerker, T., and Peter, H. H. (1995) 3'-Demethoxy-3'-hydroxystaurosporine, a novel staurosporine analog produced by a blocked mutant. *J. Antibiotics 48*, 300-305.

[41] Sheldrick, G. M. (2008) A short history of SHELX. *Acta Crystallogr. A64*, 112−122.

[42] Parsons, S., Flack, H. D., Wagner, T. (2013) Use of intensity quotients and differences in absolute structure refinement. *Acta Crystallogr. B69*, 249−259.

[43] van der Sluis, P., Spek, A. L. (1990) BYPASS: An effective method for the refinement of crystal structures containing disordered solvent regions. *Acta Crystallogr. A46*, 194-201.

[44] Barretina, J., Caponigro, G., Stransky, N., Venkatesan, K., Margolin, A. A., Kim, S., Wilson, C., Lehar, J., Kryukov, G. V., Sonkin, D., Reddy, A., Liu, M., Murray, L., Berger, M. F., Monahan, J. E., Morais, P., Meltzer, J., Korejwa, A., Valbuena, J. J., Mapa, F. A., Thibault, J., Bric-Furlong, E., Raman, P., Shipway, A., Engels, I. H., Cheng, J., Yu, G. K., Yu, J., Aspesi, P., de Silva, M., Jagtap, K., Jones, M. D., Wang, L., Hatton, C., Palescandolo, E., Gupta, S., Mahan, S., Sougnez, C., Onofrio, R. C., Liefeld, T., MacConaill, L., Winckler, W., Reich, M., Li, N., Mesirov, J. P., Gabriel, S. B., Getz, G., Ardlie, K., Chan, V., Myer, V. E., Weber, B. L., Porter, J., Warmuth, M., Finan, P., Harris, J. L., Meyerson, M., Golub, T. R., Morrissey, M. P., Sellers, W. R., Schlegel, R., and Garraway, L. A. (2012) The Cancer Cell Line Encyclopedia enables predictive modelling of anticancer drug sensitivity. *Nature 483*, 603-7.

[45] Warmuth, M., Kim, S., Gu, X., Xia, G., and Adrian, F. (2007) Ba/F3 cells and their use in kinase drug discovery. *Curr. Opin. Oncol. 19*, 55-60.

[46] O'Brien, J., Wilson, I., Orton, Terry., and Pognan, F. (2000) Investigation of the Alamar Blue (resazurin) fluorescent dye for the assessment of mammalian cell cytotoxicity. *Eur. J. Biochem. 267*, 5421-5426.

[47] Manley, P. W., Drueckes, P., Fendrich, G., Furet, P., Liebetanz, J., Martiny-Baron, G., Mestan, J., Trappe, J., Wartmann, M., and Fabbro, D. (2010) Extended kinase profile and properties of the protein kinase inhibitor nilotinib. Biochim. *Biophys. Acta, Proteins and Proteomics 1804*, 445-453.

[48] Daley, G. Q., and Baltimore, D. (1988) Transformation of an interleukin-3 dependent hematopoietic cell line by the chronic myelogenous leukemia-specific p210bcr/abl protein. *Proc. Natl Acad. Sci. USA 85*, 9312–9316.

[49]

NIHNCISurveillance,EpidemiologyandEndResultsProgram(SEER)STATfactsheets:AcuteMyeloidLeukemia(AML);https://seer.cancer.gov/statfacts/html/amyl.html

[50] Hirsch, P., Zhang, Y., Tang, R., Joulin, V., Boutroux, H., Pronier, E., Moatti, H., Flandrin, P., Marzac, C., Bories, D., Fava, F,, Mokrani, H., Betems, A., Lorre, F., Favier, R., Feger, F., Mohty, M., Douay, L., Legrand, O., Bilhou-Nabera, C., Louache, F., and Delhommeau, F. (2016) Genetic hierarchy and temporal variegation in the clonal history of acute myeloid leukaemia. *Nat. Commun. 7*, 12475.

[51] Papaemmanuil, E., Gerstung, M., Bullinger, L., Gaidzik, V. I., Paschka, P., Roberts, N. D., Potter, N. E., Heuser, M., Thol, F., Bolli, N., Gundem, G., Van Loo P., Martincorena, I., Ganly, P., Mudie, L., McLaren, S., O'Meara, S., Raine, K., Jones, D. R., Teague, J. W., Butler, A. P., Greaves, M. F., Ganser, A., Döhner, K., Schlenk, R. F., Döhner, H., and Campbell, P. J. (2016) Genomic Classification and Prognosis in Acute Myeloid Leukemia. *New Engl. J. Med. 374*, 2209-2221.

[52] Kasai, M., Yamada, R., and Omura, S. Preparation of 7-alkoxy- or 7-hydroxystaurosporine as antibacterial and antitumor agents. Patent JP 07224067, 1995.

[53] Sasaki, T., Ishii, S., Senda, M., Akinaga, S., and Murakata, C. (1996) Synthesis of [7β-methoxy 11C]methoxystaurosporine for imaging protein kinase C localization in the brain. Appl. Radiat. Isot. 47, 67-69.

[54] Kobayashi, K., Chikazawa, Y., Ezaki, K. (2015) One-pot synthesis of 3-alkoxy-2,3-dihydro-1H-isoindol-1-ones by the reactions of 2-(azidomethyl)benzoates with NaH. *Helv. Chim. Acta 98*, 604-610.

[55] Kreher, R. P., and Konrad, M. R. (1986) Chemistry of isoindoles and isoindolenines. 24. 1,3-Dimethoxy-2-methyl-2H-isoindole, a reactive o-quinoid hetarene with donor substituents in the 5-membered ring. *Chem.-Ztg. 110*, 363-367.

[56] Palmer, B. D., Thompson, A. M., Booth, R. J., Dobrusin, E. M., Kraker, A. J., Lee, H. H., Lunney, E. A., Mitchell, L. H., Ortwine, D. F., Smaill, J. B., Swan, L. M., and Denny, W. A. (2006) 4-Phenylpyrrolo[3,4-c]carbazole-1,3(2H,6H)-dione Inhibitors of the Checkpoint Kinase Wee1. Structure-Activity Relationships for Chromophore Modification and Phenyl Ring Substitution. *J. Med. Chem. 49*, 4896-4911.

[57] Zarrinkar, P. P., Gunawardane, R. N., Cramer, M. D., Gardner, M. F., Brigham, D., Belli, B., Karaman, M. W., Pratz, K. W., Pallares, G., Chao, Q., Sprankle, K. G., Patel, H. K., Levis, M., Armstrong, R. C., Joyce, J., and Bhagwat, S. S. (2009) AC220 is a uniquely potent and selective inhibitor of FLT3 for the treatment of acute myeloid leukemia (AML). *Blood 114*, 2984-2992.

[58] https://www.accessdata.fda.gov/drugsatfda_docs/nda/2017/207997Orig1Orig2s000PharmR.pdf.

[59] Nick, H. J., Kim, H., Chang, C,. Harris, K. W., Reddy, V., and Klug, C. A. (2012) Distinct classes of c-Kit-activating mutations differ in their ability to promote RUNX1-ETO-associated acute myeloid leukemia. *Blood 119*, 1522-1531.

[60] Ayatollahi, H., Shajiei, A., Sadeghian, M. H., Yazdandoust, E., Shams, S. F., Shakeri, S., Sheikhi, M., and Ghazanfarpour, M. (2017) Prognostic Importance of C-KIT Mutations in Core Binding Factor Acute Myeloid Leukemia: A Systematic Review. *Hematol. Oncol. Stem Cell Ther. 10*, 1-7.

[61] Zabkiewicz, J., Pearn, L., Hills, R. K., Morgan, R. G., Tonks, A., Burnett, A. K., and Darley, R. L. (2014) The PDK1 master kinase is over-expressed in acute myeloid leukemia and promotes PKC-mediated survival of leukemic blasts. *Haematologica 99*, 858-864.

[62] Gagliardi, P. A., Puliafito, A., and Primo, L. (2018) PDK1: At the crossroad of cancer signaling pathways. *Semin. Cancer Biol. 48*, 27-35.

[63] Alexeeva, M., Aaberg, E., Engh, R. A., and Rothweiler, U. (2015) The structure of a dual-specificity tyrosine phosphorylation-regulated kinase 1A-PKC412 complex reveals disulfide-bridge formation with the anomalous catalytic loop HRD(HCD) cysteine. *Acta Cryst. D71*, 1207-1215.

[64] Komander, D., Kular, G. S., Bain, J., Elliott, M., Alessi, D. R., and van Aalten, D. M. F. (2003) Structural basis for UCN-01 (7-hydroxystaurosporine) specificity and PDK1 (3-phosphoinositide-dependent protein kinase-1) inhibition. *Biochem J. 375*, 255-262.

[65] Zhu, X., Kim, J. L., Newcomb, J. R., Rose, P. E., Stover, D. R., Toledo, L. M., Zhao, H., Morgenstern, K. A. (1999) Structural analysis of the lymphocyte-specific kinase Lck in complex with non-selective and Src family selective kinase inhibitors. *Structure 7*, 651-661.

[66] Matsuo, Y., Drexler, H. G., Harashima, A., Okochi, A., Hasegawa, A., Kojima, K., and Orita, K.(2004) Induction of CD28 on the new myeloma cell line MOLP-8 with t(11;14)(q13;q32) expressing δ/λ type immunoglobulin. *Leukemia Res. 28*, 869-877.

[67] Spiekermann, K., Dirschinger, R. J., Schwab, R., Bagrintseva, K., Faber, F., Buske, C., Schnittger, S., Kelly, L. M., Gilliland, D. G., and Hiddemann, W. (2003) The protein tyrosine kinase inhibitor SU5614 inhibits FLT3 and induces growth arrest and apoptosis in AML-derived cell lines expressing a constitutively activated FLT3. *Blood 101*, 1494-1504.

[68] Tiacci, E., Spanhol-Rosseto, A., Martelli, M. P., Pasqualucci, L., Quentmeier, H., Grossmann, V., Drexler, H. G., and Falini, B. (2012) The NPM1 wild-type OCI-AML2 and the NPM1-mutated OCI-AML3 cell lines carry DNMT3A mutations. *Leukemia 26*, 554-557.

[69] Tan, M., Ng, I. K. S., Ban, K., Chen, Z., Ng, C., Chiu, L., Lin, M., Yan, B., Seah, E., Ng, C. H., and Chng, W. (2017) Clinical implications of DNMT3A mutations in a Southeast Asian cohort of acute myeloid leukaemia patients. *J. Clin. Pathol.70*, 669-676.

[70] Chaudry, S. F., and Chevassut, T. J. T. (2017) Epigenetic guardian: a review of the DNA methyltransferase DNMT3A in acute myeloid leukaemia and clonal haematopoiesis. *BioMed Res. Int*. 5473197/1-5473197/13.

[71] Furukawa, Y., Vu, H. A., Akutsu, M., Odgerel, T., Izumi, T., Tsunoda, S., Matsuo, Y., Kirito, K., Sato, Y., Mano, H., and Kano, Y. (2007) Divergent cytotoxic effects of PKC412 in combination with conventional antileukemic agents in FLT3 mutation-positive versus -negative leukemia cell lines. *Leukemia 21*, 1005-1014.

[72] Piloto, O., Wright, M., Brown, P., Kim, K., Levis, M., and Small, D. (2007) Prolonged exposure to FLT3 inhibitors leads to resistance via activation of parallel signaling pathways. *Blood 109*, 1643-1652.

[73] Testa, U., Pelosi, E., and Frankel, A. (2014) CD 123 is a membrane biomarker and a therapeutic target in hematologic malignancies. *Biomarker Res. 2*, 4.

[74] Baker, S. J.; Rane, S. G.; Reddy, E. P. (2007) Hematopoietic cytokine receptor signaling. *Oncogene 26*, 6724-6737.

[75] Tang, Y., Nordigarden, A., Kumar, K., Ahsberg, J., Rorby, E., Halvarsson. C., Wong, W. M., and Jonsson, J. (2015) Coexpression of hyperactivated AKT1 with additional genes activated in leukemia drives hematopoietic progenitor cells to cell cycle block and apoptosis. *Exp. Hematol. 43*, 554-64.

[76] Tang, A., Gao, K., Chu, L., Zhang, R., Yang, J., and Zheng, J. (2017) Aurora kinases: novel therapy targets in cancers. *Oncotarget 8*, 23937-23954.

[77] Goldenson, B., and Crispino, J. D. (2015) The aurora kinases in cell cycle and leukemia, *Oncogene 34*, 537-545.

[78] Park, I.-K., Mundy-Bosse, B., Whitman, S. P., Zhang, X., Warner, S. L., Bearss, D. J., Blum, W., Marcucci, G., and Caligiuri, M. A. (2015) Receptor tyrosine kinase Axl is required for resistance of leukemic cells to FLT3-targeted therapy in acute myeloid leukemia. *Leukemia 29*, 2382-2389.

[79] Gay, C. M., Balaji, K., and Byers, L. A. (2017) Giving AXL the axe: targeting AXL in human malignancy. *Br. J. Cancer 116*, 415-423.

[80] Yuan, L. L., Green, A., David, L., Dozier, C., Recher, C., Didier, C., Tamburini, J., and Manenti, S. (2014) Targeting CHK1 inhibits cell proliferation in FLT3-ITD positive acute myeloid leukemia. *Leuk. Res 38*, 1342-1349.

[81] Weir, M. C., Hellwig, S., Tan, L., Liu, Y., Gray, N. S., and Smithgall, T. E. (2017) Dual inhibition of Fes and Flt3 tyrosine kinases potently inhibits Flt3-ITD+ AML cell growth. *PLoS One 12*, e0181178.

[82] Lopez, S., Voisset, E., Tisserand, J. C., Mosca, C., Prebet, T., Santamaria, D., Dubreuil, P., and De Sepulveda, P. (2016) An essential pathway links FLT3-ITD, HCK and CDK6 in acute myeloid leukemia. *Oncotarget 7*, 51163-51173.

[83] Chapuis, N., Tamburini, J., Cornillet-Lefebvre, P., Gillot, L., Bardet, V., Willems, L., Park, S., Green, A. S., Ifrah, N., Dreyfus, F., Mayeux, P., Lacombe, C., and Bouscary, D. (2010) Autocrine IGF-1/IGF-1R signaling is responsible for constitutive PI3K/Akt activation in acute myeloid leukemia: therapeutic value of neutralizing anti-IGF-1R antibody. *Haematologica 95*, 415-423.

[84] Karmali, R., Larson, M. L., Shammo, J. M., Basu, S., Christopherson, K., Borgia, J. A., and Venugopal, P. (2015) Impact of insulin-like growth factor 1 and insulin-like growth factor binding proteins on outcomes in acute myeloid leukemia. *Leuk. Lymph 56*, 3135-3142.

[85] Furqan, M., Mukhi, N. Lee, B., and Liu, D. (2013) Dysregulation of JAK-STAT pathway in hematological malignancies and JAK inhibitors for clinical application. *Biomarker Res 1*, 5.

[86] Robinson, L. J., Xue, J., and Corey, S. J. (2005) Src family tyrosine kinases are activated by Flt3 and are involved in the proliferative effects of leukemia-associated Flt3 mutations. *Exp. Hematol 33*, 469-479.

[87] Dos Santos, C., Demur, C., Bardet, V., Prade-Houdellier, N., Payrastre, B., and Récher, C. (2008) A critical role for Lyn in acute myeloid leukemia. *Blood 111*, 2269-2279.

[88] Leischner, H., Albers, C., Grundler, R., Razumovskaya, E., Spiekermann, K., Bohlander, S., Rönnstrand, L., Götze, K., Peschel, C., and Duyster, J. (2012) SRC is a signaling mediator in FLT3-ITD but not in FLT3-TKD–positive AML. *Blood 119*, 4026-4033.

[89] Fathi, A. T., Arowojolu, O., Swinnen, I., Sato, T., Rajkhowa, T., Small, D., Marmsater, F., Robinson, J. E., Gross, S. D., Martinson, M., Allen. S., Kallan, N. C., and Levis, M. (2012) A potential therapeutic target for FLT3-ITD AML: PIM1 kinase. *Leukemia Res. 36*, 224-231.

[90] Garcia, P. D., Langowski, J. L., Wang, Y., Chen, M., Castillo, J., Fanton, C., Ison, M., Zavorotinskaya, T., Dai, Y., Lu, J., Niu, X., Basham, S., Chan, J., Yu, J., Doyle, M., Feucht, P., Warne, R., Narberes, J., Tsang, T., Fritsch, C., Kauffmann, A., Pfister, E., Drueckes, P., Trappe, J., Wilson, C., Han, W., Lan, J., Nishiguchi, G., Lindvall, M., Bellamacina, C., Aycinena, J. A., Zang, R., Holash, J., and Burger, M. T. (2014) Pan-PIM Kinase Inhibition

Provides a Novel Therapy for Treating Hematologic Cancers. *Clin. Cancer Res.20*, 1834-1845.

[91] Green, A. S., Maciel, T. T., Hospital, M., Yin, C., Mazed, F., Townsend, E. C., Pilorge, S., Lambert, M., Paubelle, E., Jacquel, A., Zylbersztejn, F., Decroocq, J., Poulain, L., Sujobert, P., Jacque, N., Adam, K., So, J. C. C., Kosmider, O., Auberger, P., Hermine, O., Weinstock, D. M., Lacombe, C., Mayeux, P., Vanasse, G. J., Leung, A. Y., Moura, I. C., Bouscary, D., and Tamburini, J. (2015) Pim kinases modulate resistance to FLT3 tyrosine kinase inhibitors in FLT3-ITD acute myeloid leukemia. *Sci. Adv. 1*, e1500221.

[92] Janning, M., and Fiedler, W. (2014) Volasertib for the treatment of acute myeloid leukemia: a review of preclinical and clinical development. *Future Oncol.10*, 1157-1165.

[93] Barabe, F., Gil, L., Celton, M., Bergeron, A., Lamontagne, V., Roques, E., Lagace, K., Forest, A., Johnson, R., Pecheux, L., Simard, J., Bellemare-Pelletier, A., Gagnon, E., Hébert, J., Cellot, S., and Wilhelm, B. T. (2017) Modeling human MLL-AF9 translocated acute myeloid leukemia from single donors reveals RET as a potential therapeutic target. *Leukemia 31*, 1166-1176.

[94] Rudat, S., Pfaus, A., Bühler, C., Rabe, S., Bullinger, L., Gröschel, S., Sykes, S. M., Milsom, M. D., Ellegast, J. M., Fröhling, S., and Scholl, C. (2016) The RET Receptor Tyrosine Kinase Promotes Acute Myeloid Leukemia through Protection of FLT3-ITD Mutants from Autophagic Degradation. *Blood 128*, Abstr 2849.

[95] Puissant, A., Fenouille, N., Alexe, G., Pikman, Y., Bassil, C. F., Mehta, S., Du, J., Kazi, J. U., Luciano, F., Roonstrand, L., Kung, A. L., Aster, J. C., Galinsky, I., Stone, R. M., DeAngelo, D. J., Hemann, M. T., and Stegmaier, K. (2014) SYK is a critical regulator of FLT3 in acute myeloid leukemia. *Cancer Cell 25*, 226-42.

[96] Meyer, J., Rhein, M., Schiedlmeier, B., Kustikova, O., Rudolph, C., Kamino, K., Neumann, T., Yang, M., Wahlers, A., Fehse, B., Reuther, G. W., Schlegelberger, B., Ganser, A., Baum, C., and Li, Z. (2007) Remarkable leukemogenic potency and quality of a constitutively active neurotrophin receptor, ΔtrkA. *Leukemia 21*, 2171-2180.

[97] Cogle, C. R., Bosse, R. C., Brewer, T., Migdady, Y., Shirzad, R., Kampen, K. R., and Saki, N. (2016) Acute myeloid leukemia in the vascular niche. *Cancer Lett. 380*, 552-560.

[98] Apperley, J. F. (2007) Part I: Mechanisms of resistance to imatinib in chronic myeloid leukemia. *Lancet Oncol. 8*, 1018-1029.

[99] Holohan, C., Van Schaeybroeck, S., Longley, D. B., and Johnston, P. G. (2013) Cancer drug resistance: an evolving paradigm. *Nat. Rev. Cancer 13*, 714-726.

[100] Cree I. A., and Charlton, P. (2017) Molecular chess? Hallmarks of anti-cancer drug resistance. *BMC Cancer 17*, 10.

[101] Cowan-Jacob, S. W., Guez, V., Fendrich, G., Griffin, J. D., Fabbro, D., Furet, P., Liebetanz, J., Mestan, J., and Manley, P. W. (2004) Imatinib (STI571) Resistance in Chronic Myelogenous Leukemia: Molecular Basis of the Underlying Mechanisms and Potential Strategies for Treatment. *Mini-Rev. Med. Chem. 4*, 285-299.

[102] Tiedt, R., Degenkolbe, E., Furet, P., Appleton, B. A., Wagner, S., Schoepfer, J., Buck, E., Ruddy, D. A., Monahan, J. E., Jones, M. D., Blank, J., Haasen, D., Drueckes, P., Wartmann, M., McCarthy, C., Sellers, W. R., and Hofmann, F. (2011) A Drug Resistance Screen Using a Selective MET Inhibitor Reveals a Spectrum of Mutations That Partially Overlap with Activating Mutations Found in Cancer Patients. *Cancer Res.71*, 5255-5264.

[103] Cools, J., Mentens, N., Furet, P., Fabbro, D., Clark, J. J., Griffin, J. D., Marynen, P., and Gilliland, D. G. (2004) Prediction of Resistance to Small Molecule FLT3 Inhibitors:

Implications for Molecularly Targeted Therapy of Acute Leukemia. *Cancer Res. 64*, 6385-6389.

[104] von Bubnoff, N., Engh, R. A., Aaberg, E., Saenger, J., Peschel, C., and Duyster, J. (2009) FMS-Like Tyrosine Kinase 3-Internal Tandem Duplication Tyrosine Kinase Inhibitors Display a Nonoverlapping Profile of Resistance Mutations In vitro. *Cancer Res. 69*, 3032-3041.

[105] Albers. C., Leischner, H., Verbeek, M., Yu, C., Illert, A. L., Peschel, C., von Bubnoff, N., and Duyster, J. (2013) The secondary FLT3-ITD F691L mutation induces resistance to AC220 in FLT3-ITD+ AML but retains in vitro sensitivity to PKC412 and sunitinib. *Leukemia 27*, 1416-1418.

[106] Weisberg, E., Ray, A., Nelson, E., Adamia, S., Barrett, R., Sattler, M., Zhang, C., Daley, J. F., Frank, D., Fox, E., and Griffin, J. D. (2011) Reversible resistance induced by FLT3 inhibition: a novel resistance mechanism in mutant FLT3-expressing cells. *PLoS One 6*, e25351.

[107] Stolzel, F., Steudel, Christine., Oelschlagel, U., Mohr, B., Koch, S., Ehninger, G., and Thiede, C. (2010) Mechanisms of resistance against PKC412 in resistant FLT3-ITD positive human acute myeloid leukemia cells. *Ann. Hematol. 89*, 653-662.

[108] Heidel, F., Solem, F. K., Breitenbuecher, F., Lipka, D. B., Kasper, S., Thiede, M. H., Brandts, C., Serve, H., Roesel, J., Giles, F., Feldman, E., Ehninger, G., Schiller, G. J., Nimer, S., Stone, R. M, Wang, Y., Kindler, T., Cohen, P. S., Huber, C., and Fischer, T. (2006) Clinical resistance to the kinase inhibitor PKC412 in acute myeloid leukemia by mutation of Asn-676 in the FLT3 tyrosine kinase domain. *Blood 107*, 293-300.

[109] Smith, C. C., Wang, Q., Chin, C., Salerno, S., Damon, L. E., Levis, M. J., Perl, A. E., Travers, K. J., Wang, S., Hunt, J. P., Zarrinkar, P. P., Schadt, E. E., Kasarskis, A., Kuriyan, J.,

and Shah, N. P. (2012). Validation of ITD mutations in FLT3 as a therapeutic target in human acute myeloid leukemia. *Nature 485*, 260-263.

[110] Pauwels, D., Sweron, B., and Jan Cools, J. (2012) The N676D and G697R mutations in the kinase domain of FLT3 confer resistance to the inhibitor AC220. *Haematologica 97*, 1773-1774.

[111] Zorn, J. A., Wang, Q., Fujimura, E., Barros, T., and Kuriyan, J. (2015) Crystal structure of the FLT3 kinase domain bound to the inhibitor quizartinib (AC220). *PLoS One 10*, e0121177.

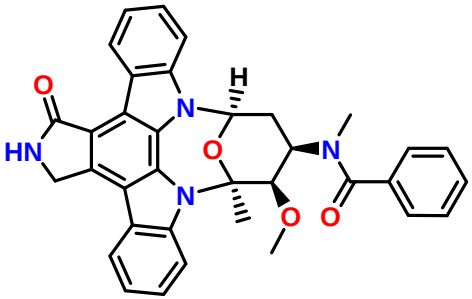

Midostaurin (N-benzoyl-staurosporin)